COMMUNICATIONS ON PURE AND APPLIED MATHEMATICS, VOL. V, 301–348 (1952)

The Flow Pattern of a Supersonic Projectile

By G. B. WHITHAM

*University of Manchester, England**

Summary

A complete first approximation is given of the supersonic flow past any slender, axisymmetrical body-wake combination, whose meridian section may have discontinuities in slope. A hypothesis, which is amply substantiated, is made that the failures of linearized theory for a description of the flow pattern may be corrected by replacing the approximate characteristics in that theory by the exact characteristics (or at least by a sufficiently good approximation to the exact ones); the ideas involved are described in the introduction (Part 1) since they are of general application, and the mathematical details for the projectile are furnished in Parts 2 and 3. To complete the description of the flow, the shocks, which occur in regions where the characteristics would otherwise form a limit line and the solution cease to be single-valued, are determined (Part 4) from the simple geometrical property that, to a first order in its strength, a shock bisects the angle between the characteristics on each side of it. This condition proves extremely powerful in the mathematical analysis, and it has additional value in that it also gives a simple qualitative picture of how the shocks occur and fit into the pattern. The general theory is applied in Part 5 to the typical example of the 5–10 calibre ogival headed bullet with a suitable wake. In Part 6, the value of the pressure at any point of the fluid is determined, and, in Part 7, the way in which the drag is related to the rate of increase of the energy of the fluid is investigated. The latter leads to an interesting new expression for the von Karman drag in terms of a function which is fundamental to the whole theory. Finally, in the Appendix, the corresponding theory for the two-dimensional steady and one-dimensional unsteady flows is set out since it gives some new information on these topics. Probably the most important result obtained in the Appendix is in the problem of a piston which oscillates periodically. It is found that, at a large distance from the piston, the strengths of the shocks depend only on the properties of the fluid, the distance from the piston and the period of the oscillation; they are independent of the particular piston motion.

1. *Introduction*

A mathematical theory is given of the disturbance produced in the surrounding air by a projectile moving with supersonic speed. A solution of the flow

*Now at New York University.

inside the wake is not obtained; its mean boundary is assumed to be known and it is the flow past the given body-wake combination which is described. The theory is first written out assuming that the body[1] is axisymmetrical, slender and pointed at the nose (with the Mach number sufficiently in excess of 1 for the front shock to be attached), although discontinuities in the slope of the meridian section are allowed; then a *complete* first approximation to the whole flow pattern is given. If some of these conditions are not satisfied, the description is not complete but, as will be explained later, many important results can be taken over to these cases without modification.

Valuable information of the shape of the wake and a picture of the shocks which occur in the flow are provided by photographs of bullets in flight; the basic flow pattern is sketched in Figure 1. At the base of the projectile there is a

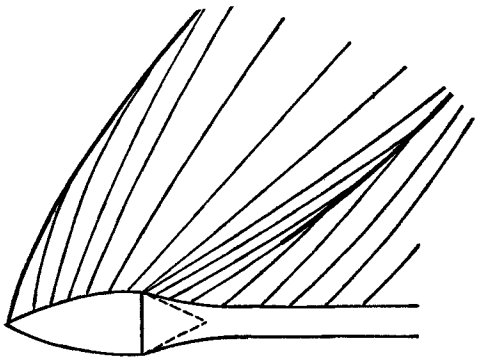

FIGURE 1

roughly conical dead air region at a lower pressure so that the stream expands sharply round the base; a typical value for the angle through which it turns is 12°. But then, the stream is recompressed as the boundary layer between it and the dead air region thickens to form the turbulent wake of roughly constant cross-section. Fluctuations of the wake boundary due to the turbulence inside will not affect the main features of the flow and are ignored. Turning now to the flow pattern, there is an attached front shock which curves round towards the undisturbed Mach direction and weakens as the distance from the body increases; ahead of it the flow is undisturbed. At the rear, there will always be a second shock (this would be true even if the wake were taken to be of constant cross-section equal to the base of the body). A rear shock is immediately more difficult to deal with than the front one since there is a non-uniform state on *both* sides of it, but in addition, further complications arise in that more than one shock may be formed, particularly if there are discontinuities in the slope of the meridian section (although not only in such cases). Thus, there may be a shock system at the rear consisting of several shocks, ultimately running together to

[1]The term "body" will henceforth be used to include the wake.

form the main shock which decays in a similar way to the front one. The prediction and description of such a complex shock system forms the most fascinating part of the theory.

The corresponding problem of two dimensional supersonic flow past an aerofoil was solved by Friedrichs [1]. The theory is considerably easier since a solution of the exact equations of the isentropic flow is already known, i.e. the so-called "simple wave", and it is only necessary to fit on the shocks in a suitable manner. Moreover the determination of the shocks themselves is less complicated since Friedrichs assumes that there are just single shocks attached to the leading and trailing edges, respectively, and that the flow behind the rear shock is undisturbed. If the aerofoil section has no compressive discontinuities in slope and is pointed at each end, this is a good approximation to the truth[2]; hence discussion of the formation of a shock *inside* a disturbed region is avoided in this case. However, it is more important in the analogous unsteady problems of one dimensional plane waves which Friedrichs also treats, and in these problems he does consider shock formation inside a wave, but is only able to obtain the details of the shock near the point of formation; he cannot go on to describe its ultimate decay, for example. Now, these problems can be solved by the methods of this paper and so, although its main objective is the projectile problem, the corresponding theory for two-dimensional flow (and the analogous one dimensional wave problems) in which the flow pattern for *any* thin aerofoil section is described, is set out briefly in the Appendix. Of course this theory would only give the first approximation whereas the Friedrichs theory, with a certain modification which is described in the next paragraph, is correct to a second order; thus the present method loses some accuracy but penetrates further.

The question of the accuracy of Friedrichs' theory raises a very important point. That theory and also the theory which will be described for the axisymmetrical problem, use solutions of the isentropic equations of motion to describe the flow and then the occurrence and positions of curved shocks are determined from them. This procedure has been criticised on the grounds of inconsistency since curved shocks are of non-uniform strength and the flow behind is therefore not isentropic. The explanation is that the isentropic equations of motion are used not because it is assumed that the flow is exactly isentropic, but because it is thought that they will give a good approximation to the correct (non-isentropic) one since the shocks concerned are weak and the entropy changes at a shock are of the third order in its strength. In order to clarify the position and put this extremely general and valuable approach on a firm basis, Lighthill [2] has investigated the accuracy of Friedrichs' theory and applied a comprehensive check on its results. He finds that the theory is correct to the second order (as expected) with one important exception: the position of the rear shock is

[2]It would not be so for a body of revolution satisfying these conditions since even on linearized theory, the flow behind the body is not uniform (the "tail" of a cylindrical sound pulse).

correct only to a first order. This is due to a wide third order pressure wave, spread out behind the main disturbance, which interacts with the rear shock over a large distance to modify its position. The pressure wave is determined and the results for the rear shock are corrected. The knowledge of the validity of the approach in Friedrichs' work justifies its use in other problems, since a similar behaviour is expected. Thus in the flow past the projectile strictly similar effects may be sketched in but in this paper, since only the first order flow pattern is obtained they will not appear in the analysis.

For the axisymmetrical flow past a projectile no exact solution of the equations of motion is available, so that the first step in this theory is to provide a valid description of the non-linear flow. The existing linearized theory is now well-known (see, for example, Lighthill [3]), but it is easily seen to be inadequate, as it stands, for a detailed description of the flow outlined above. In it the disturbance is propagated diagonally downstream along straight parallel characteristics $x - r\sqrt{(M^2 - 1)} = \text{constant}$, where x is the distance along the axis from the nose, r the distance from the axis and M the Mach number of the main stream. This is obviously incorrect since, in fact, the disturbed region spreads out with curved characteristics which ultimately diverge (see Figure 1). Moreover, the shocks, whose presence in the correct theory is most important, are entirely absent since they are a non-linear phenomenon; for example, in the linearized solution, the flow is uniform ahead of the leading characteristic $x - r\sqrt{(M^2 - 1)} = 0$ whereas it is known that the front shock is there. The same failures occur in Broderick's further approximations [4], since his reduction of the equations to a series of linear ones avoids the essential non-linearity of the problem. However, in spite of this criticism, these theories are extremely valuable because (i) they do give valid approximations to the pressure forces acting on the body, and (ii) (much more important from the present point of view) *the failure of the linear theory as a description of the flow can be remedied.* The modified linear theory forms the basis of the work. It is the solution, in this problem, corresponding to the "simple wave" used in Friedrichs' work; in fact, when the method is applied to the two-dimensional flow (see Appendix) it does give the first approximation to the "simple wave." From it the theory is developed as outlined in the summary.

The ideas which have culminated in this theory arose from the author's previous work on the problem [5]. In this work, a direct attack was made on the exact equations of motion but to make the task less formidable, the discussion was limited to the behaviour at large distances. A solution was found as a series in descending powers of r and it was noticed that, for the case of a slender body when the disturbance could be assumed to be small from the outset and hence certain terms neglected, the solution had the same *form* as the expansion of the linearized one except that the approximate characteristic variable $x - r\sqrt{(M^2 - 1)}$ was replaced therein by the exact one $y(x, r)$ such that $y = \text{constant}$ is an exact characteristic curve. Hence it was deduced that the only failure of linearized theory at large distances is that the characteristics in it are incorrect. The

only real use made of this interesting fact was that, by comparison, the arbitrary function and constants appearing in the general theory were obtained in terms of the body shape; the full meaning and the possibility of its application in a general way were not appreciated. Now it becomes the starting point of the whole theory; the fundamental hypothesis is made that linearized theory gives a valid first approximation to the flow *everywhere* provided that in it the approximate characteristics are replaced by the exact ones, or at least by a sufficiently good approximation to the exact ones. (A more precise statement is given with the mathematical details in Part 2.)

An examination of the underlying physical ideas reveals the reasons for making this hypothesis. Linearized theory is essentially an acoustic one in that disturbances are propagated at a *constant* speed equal to the speed of sound in the main stream; it does not take account of the variation in the local speed of sound or of the convection of sound with the moving fluid. It is permissible to use such a theory to describe the propagation of disturbances in very small regions; but if they are to be combined into a complete picture, the appropriate local speed of propagation which is equal to the local speed of sound plus the local fluid velocity, must be used in each region, otherwise the error accumulates. Thus it is expected that the linearized theory has the correct variation of physical quantities along the characteristics, which trace the paths of the wave fronts, but has the wrong curves for the characteristics. The hypothesis is designed to adjust this. Apart from the physical interpretation, the theory is amply substantiated by the checks that can be made in several places of its correct prediction of certain results that are already known by other methods. Among these checks, there is the complete reproduction of the results at large distances which were found previously, and others will be remarked as they arise. Finally, exactly the same procedure in the problems which are discussed by Friedrichs yields the first approximation to his results. Thus there can be little doubt of the validity of the hypothesis.

It is assumed in the theory that the body is slender and pointed at the nose, with the front shock attached, but even if these conditions are not satisfied it may still be used to deduce the behaviour of the flow at large distances. For, certainly at a sufficient distance from the body the disturbance will be small. Therefore, consider a stream tube with radius so large that its deviation from a cylinder of constant radius is very small. Then the problem of the flow outside is that of the flow past a quasi-cylindrical duct and it may be described by the theory of this paper, and hence the similar results at large distances obtained. In this case, of course, the arbitrary function occurring in the solution remains undetermined since it depends on the shape of the stream tube which is unknown unless the flow near the body is solved. This is in agreement with the previous work [5] since then the arbitrariness could only be resolved when the body was slender and the general theory linked up with the shape of the body by means of linear theory. Thus the present theory entirely replaces the previous paper; it is much fuller, it includes all the "large distance" results and is obtained much

more quickly and easily since the exact equations of motion are now avoided. The other restrictive condition is that of axial symmetry. Suppose that this condition is relaxed but that the body is slender and pointed at the nose (with attached shock). The linearized theory of this problem has been given by Ward [6], and it is found that the flow becomes axisymmetrical when $r\sqrt{(M^2-1)}/\{x - r\sqrt{(M^2-1)}\}$ is not small. The quantity $x - r\sqrt{(M^2-1)}$ is the linearized form of the characteristic variable and measures the distance from the nose at which the characteristic starts; hence the condition is, correctly interpreted, that at any point the distance from the axis divided by the distance from the nose at which the characteristic surface (on which the point lies) started from the body, should not be small. This is clearly satisfied at large distances, but it is also true at points on the front shock; they are effectively at large distances because the appropriate characteristic surfaces arise so very close to the nose. (Considerable use is also made of this in the axisymmetrical case; it is discussed in more detail in Part 4.) Hence the results for the front shock and all the theory at large distances apply unchanged to the non-axisymmetrical slender body. From these extensions, it seems reasonable to suggest that the results for large distances apply to the supersonic flow past *any* finite body. These results are (see Parts 4 and 6) that there are two main shocks whose equations are approximately $x = r\sqrt{(M^2-1)} - br^{1/4}$ and $x = r\sqrt{(M^2-1)} + b_1 r^{1/4}$, where b and b_1 are constants depending on the body shape. The strengths fall off like $r^{-3/4}$ and at points between the shocks the pressure falls linearly with time at a rate $0.2\sqrt{(1-M^{-2})}\, r^{-1}$atmospheres/millisec (where r is measured in metres) which is independent of the body shape.

Before proceeding to the detailed theory, it is of interest to consider the applications of the method presented here to other problems. In principle at least, the method is extremely simple, the main reason for this being that the non-linear equations of motion are avoided, although the geometrical treatment of the shocks by the "angle property" adds much to the simplicity of its application. Moreover, since the means by which the linearized theory is rectified is of a general nature, it is hoped that this new approach will prove to be of value in other problems of research. It is immediately applicable to the connected problems of fluid flow in which there are only two independent variables. The one-dimensional unsteady waves and the two-dimensional steady supersonic flow (already discussed by Friedrichs) have been mentioned. Others which are easily solved are the problems of unsteady waves with cylindrical or spherical symmetry. The latter of these is of practical interest in explosions but since in explosions a very large disturbance of the air is desired (projectiles are designed to have the opposite effect), only the behaviour the theory gives at large distances would be of value. Hence there is little of practical importance to be added to the author's paper [7] on the subject, although the work could now be considerably shortened, and for scientific interest a very weak explosion could be described completely. The author hopes to solve other problems involving two independent variables, where the only difficulty is the application of the method, and also to

develop a similar technique for problems involving three independent variables.

In the account of the work many figures are necessary; they are of two types: First there are sketches which form part of the explanation of the text; in order to make the essential details clear they are not drawn in correct proportion (for example, distances in the Mach direction are very large and therefore sketches of the flow plane are contracted in this direction). These figures are numbered and are inserted in the text at the appropriate points. Secondly, there are graphs which show the results of numerical calculations, and may be referred to throughout the paper; because of their different nature these are collected separately at the end of the paper.

2. *Improvement of Linearized Theory*

Let the steady stream have velocity U in the x-direction, and at a general point (x, r) let the velocity be $(U + Uu, Uv)$. The flow is assumed to be irrotational hence the perturbation velocities u and v may be deduced from a potential ϕ which, on the linearized theory, satisfies the equation

$$\phi_{rr} + \frac{1}{r}\phi_r - \alpha^2\phi_{xx} = 0, \tag{1}$$

where $\alpha = \sqrt{(M^2 - 1)}$ and suffixes denote partial differentiation. The solution of (1) which represents a disturbance propagated downstream from a body is

$$\phi = -\int_0^{x-\alpha r} \frac{f(t)\,dt}{\sqrt{(x-t)^2 - \alpha^2 r^2}}, \tag{2}$$

giving

$$u = -\int_0^{x-\alpha r} \frac{f'(t)\,dt}{\sqrt{(x-t)^2 - \alpha^2 r^2}}, \tag{3}$$

$$v = \frac{1}{r}\int_0^{x-\alpha r} \frac{(x-t)f'(t)\,dt}{\sqrt{(x-t)^2 - \alpha^2 r^2}}; \tag{4}$$

the downstream characteristics of the equation are $x - \alpha r =$ constant. The arbitrary function $f(x)$ is determined from the boundary condition on the body and will be dealt with in detail in the next paragraph.

The method by which linearized theory must be modified has been described in the introduction and is embodied in the following precise hypothesis. *Linearized theory gives a correct first approximation everywhere provided that the value which it predicts for any physical quantity, at a given distance r from the axis on the approximate characteristic $x - \alpha r =$ constant, pointing downstream from a given point on the body surface, is interpreted as the value, at that distance from the axis, on the exact characteristic which points downstream from the said point.* Carrying out the modification, u and v become, replacing $x - \alpha r$ by $y(x, r)$,

$$u = -\int_0^y \frac{f'(t)\,dt}{\sqrt{(y-t)(y-t+2\alpha r)}}, \tag{5}$$

$$v = \frac{1}{r}\int_0^y \frac{(y-t+\alpha r)f'(t)\,dt}{\sqrt{(y-t)(y-t+2\alpha r)}}; \tag{6}$$

y is now determined from the condition that $y(x, r) =$ constant is a characteristic curve, that is, along it $dx/dr = \cot(\mu + \theta)$, where μ is the local Mach angle and θ is the local direction of flow. The local velocity of sound, a, is determined from Bernoulli's equation,

$$\frac{a^2}{\gamma-1} + \tfrac{1}{2}U^2\{(1+u)^2 + v^2\} = \frac{a_0^2}{\gamma-1} + \tfrac{1}{2}U^2, \tag{7}$$

where suffix 0 refers to the value in the undisturbed stream and γ is the ratio of the specific heats, hence

$$\mu = \sin^{-1}\frac{a}{q} = \mu_0 - \left(1 + \frac{\gamma-1}{2}M^2\right)\alpha^{-1}u + O(u^2+v^2), \tag{8}$$

where q is the magnitude of the velocity. The stream direction θ is given by $\tan^{-1}\{v/(1+u)\} = v + O(u^2+v^2)$. Therefore, on $y =$ constant,

$$\frac{dx}{dr} = \alpha + \frac{(\gamma+1)M^4}{2\alpha}u - M^2(v+\alpha u) + O(u^2+v^2). \tag{9}$$

The value of y on a characteristic has not been defined uniquely, although on the body it must be approximately equal to $x - \alpha r$ (which it replaces in linearized theory); it is now made quite definite by taking it *equal* to the value of $x - \alpha r$ at the point where the characteristic meets the body surface.[3] Then, substitution of (5) and (6) in (9) gives, on performing the integration,

$$\begin{aligned} x = \alpha r &- \frac{(\gamma+1)M^4}{2\alpha^2}\int_0^y \left\{\frac{\sqrt{y-t+2\alpha r} - \sqrt{y-t+2\alpha R(y)}}{\sqrt{y-t}}\right\} f'(t)\,dt \\ &- 2M^2\int_0^y \log\left\{\frac{\sqrt{y-t+2\alpha r} - \sqrt{y-t}}{\sqrt{y-t+2\alpha r} + \sqrt{y-t}}\right. \\ &\left.\cdot\frac{\sqrt{y-t+2\alpha R(y)} + \sqrt{y-t}}{\sqrt{y-t+2\alpha R(y)} - \sqrt{y-t}}\right\} f'(t)\,dt + y \\ &= \alpha r - c(y, r) + y, \end{aligned} \tag{10}$$

say, where $R(x)$ is the radius of the body. The expression (10) determines $y(x, r)$ only approximately, since in (9) terms $O(u^2+v^2)$ have been neglected

[3] It is convenient, however, to think of y as being approximately the distance x from the nose, where the characteristic produced meets the axis.

and the first order approximations (5), (6) substituted. But, unlike linearized theory which takes $y = x - \alpha r$, thus neglecting a term which becomes infinitely large compared to $x - \alpha r$ both at large distances and near the leading Mach cone (see (12)), this is a valid approximation since the terms neglected really are small compared to those retained. Equations (5), (6) and (10) now describe the solution.

This equation for the characteristics, which determines $y(x, r)$, is extremely complicated and fortunately it is not necessary to make use of it in this form. In general only the approximation for $\alpha r/y$ large is required. Then the expressions (5), (6) and (10) become

$$u = -\frac{F(y)}{\sqrt{2\alpha}} r^{-1/2}, \qquad v = -\alpha u, \tag{11}$$

$$x = \alpha r - kF(y)r^{1/2} + y, \tag{12}$$

where

$$F(y) = \int_0^y \frac{f'(t)\,dt}{\sqrt{y - t}} \tag{13}$$

and

$$k = 2^{-1/2}(\gamma + 1)M^4\alpha^{-3/2}.$$

Taking $\gamma = 1.4$, a graph of the variation of k with Mach number M is given in Graph A. The function $F(y)$ is fundamental to the whole theory and is the most important function associated with flow past a body of revolution, as will be seen. The next paragraph is devoted to its determination from the given body shape, and to a consideration of its properties.

It should be noted that, as far as the value of the physical quantities u and v are concerned, nothing is gained by preferring (10) to (12), since when $\alpha r/y$ is not large, both $c(y, r)$ and $kF(y)r^{1/2}$ are small and the differences they make in (5) and (6) are of the same order as terms already neglected there. Hence for the physical quantities, the value of y determined by (12) may be used everywhere. However (10) still provides the correct approximation to the characteristic curves near the body; this will be used later.

It may be mentioned as additional support for the theory that (11) and (12) are in agreement with the general principle, deduced by Lighthill in §6 of his paper [8].

3. *The Function F(y)*

The arbitrary function $f(x)$ is determined by application of the boundary condition that the normal velocity at the body surface is zero. This condition when linearized becomes $v = R'(x)$ on $r = R(x)$, where $R(x)$ is the body radius at a distance x from the nose. In the most well known form of the linearized

theory, it is assumed that the body is sufficiently smooth ($S'(x)$ continuous at least) for the expression (4) for v to be approximated as $f(x)/r$ when r is small, hence the boundary condition gives

$$f(x) = R(x)R'(x) = S'(x)/2\pi,$$

so that from (13),

$$F(y) = \frac{1}{2\pi}\int_0^y \frac{S''(t)\,dt}{\sqrt{y-t}}. \tag{14}$$

If $S'(x)$ and $S''(x)$ are continuous and $O(\delta^2)$ then the error in using this value of $f(x)$ and hence the error in $F(y)$ is $O(\delta^4 \log 1/\delta)$ (see [3]), where δ is the thickness ratio; under these conditions the body will be said to be "smooth" and the simple form (14) will be used. If $S''(x)$ has discontinuities, (14) still gives some approximation and its accuracy and limitations may be investigated directly as in the previous case but this will not be done here. It is easier and more instructive to see when the general expression, which must be found in any case to apply when $S'(x)$ is discontinuous, may be reduced to (14).

The linearized theory for a body with discontinuities of slope has been given by Lighthill [9] and in fact the author is indebted to Professor Lighthill for suggesting the expression for $F(y)$ which must be used in this case. The "discontinuity theory" makes use of the powerful Heaviside calculus in which the operation $\int_0^x dx$ is represented symbolically by p^{-1}. Then (2), (3) and (4) become

$$\begin{aligned} \phi &= -K_0(\alpha pr)f(x), \\ u &= -pK_0(\alpha pr)f(x), \\ v &= -\alpha pK_0'(\alpha pr)f(x) = \alpha pK_1(\alpha pr)f(x), \end{aligned} \tag{15}$$

where K_0 and K_1 are the Bessel functions as defined by Watson. Application of the boundary condition yields

$$R'(x) = [\alpha pK_1(\alpha pr)f(x)]_{r=R(x)}, \tag{16}$$

and although this gives a formal relation for $f(x)$ its interpretation is difficult in general because $[K_1(\alpha pr)]_{r=R(x)}$ cannot simply be replaced by $K_1(\alpha pR(x))$, (the latter would allow the operators to act on $R(x)$ and this is not intended). If the body is *smooth* it is permissible in (16) to use the expansion $K_1(\alpha pr) \sim (\alpha pr)^{-1}$ for αpr small since a formal rule of Heaviside calculus is that in such an expression αpr behaves like $\alpha r/x$ (which *formally* it represents) in that if $\alpha r/x$ is small then the expression in question may be expanded for αpr small, and $\alpha r/x$ is small on the body. Hence $\alpha pK_1(\alpha pr)f(x) \sim f(x)/r$ and (16) gives $f(x) = R(x)R'(x)$. But, if the body has a discontinuity of slope at $x = t_1$, αpr behaves in the expression like $\alpha r/(x - t_1)$ which is small only away from the discontinuity; hence some other approach is required. If the problem were that of flow outside

a quasi-cylindrical duct with $R(x)$ approximately constant there would be no difficulty; (16) would give immediately

$$f(x) = \frac{1}{\alpha p R K_1(\alpha p R)} \frac{S'(x)}{2\pi}. \tag{17}$$

This suggests that if in the case of the projectile the body is divided into small intervals $x = t_i$, $i = 1, 2, 3, \cdots$, the contribution to $f(x)$ of the increment $\Delta S'(t_i)$ in $S'(x)$ in the i-th interval, is

$$f_i(x) = \frac{1}{\alpha p R_i K_1(\alpha p R_i)} \frac{\Delta S'(t_i)}{2\pi} H(x - t_i), \tag{18}$$

where $R(t_i) \equiv R_i$ and $H(x)$ is the Heaviside unit step function. Now $f(x)$ is taken to be $\sum f_i(x)$ and it may be verified that the boundary condition (16) is satisfied. For at $x = t_n$, say, the contribution of $f_i(x)$ to the right hand side of (16) is

$$\frac{K_1(\alpha p R_n)}{R_i K_1(\alpha p R_i)} \frac{\Delta S'(t_i)}{2\pi} H(x - t_i). \tag{19}$$

If t_i is not near t_n so that $\alpha R_n/(t_n - t_i)$ is small the expansions of the Bessel functions for small argument can be used as for the smooth body, and (19) is approximately $\Delta S'(t_i)/R_n$; if t_i is near t_n so that $(R_n - R_i)/R_n$ is small, (19) is again approximately $\Delta S'(t_i)/R_n$. Now for all the t_i, one of these conditions holds, because if $(t_n - t_i) = O(\alpha R_n)$ then $R(t_n) = R(t_i + O(\alpha R_n)) = R(t_i) + O(\alpha R'(t_i) R_n)$, that is $(R_n - R_i)/R_n = O(\alpha R_i')$ which is small by definition of a slender body, hence (19) is $\Delta S'(t_i)/R_n$ for all i and clearly (16) is satisfied by the sum. Essentially the method is a combination of the methods used for the smooth body and the duct; away from the discontinuities the former can be used with its expansions for small $\alpha p R$, whilst near a discontinuity $R(x)$ is approximately constant and the duct expressions apply. Thus $f(x)$ is the sum over i of the terms given by (18). If $g(x)$ represents $\{pK_1(p)\}^{-1} H(x)$ then $f_i(x) = g\{(x - t_i)/\alpha R_i\} \Delta S'(t_i)/2\pi$, hence summing over i and taking the limit,

$$f(x) = \int_0^\infty g\left(\frac{x - t}{\alpha R(t)}\right) \frac{dS'(t)}{2\pi}. \tag{20}$$

The properties of $g(x)$ and $f(x)$ can be discussed in detail by the methods used below but it is unnecessary in this work since the important function is $F(x) = \pi^{1/2} p^{1/2} f(x)$. The value of F is found similarly to f by summing the contributions from (18) and taking the limit, and is

$$F(y) = \int_0^\infty \left(\frac{2}{\alpha R(t)}\right)^{1/2} h\left(\frac{y - t}{\alpha R(t)}\right) \frac{dS'(t)}{2\pi}, \tag{21}$$

where

$$h(x) = \sqrt{\frac{\pi}{2p}} \frac{1}{K_1(p)} H(x). \tag{22}$$

Expressions (20) and (21) are Stieltjes integrals and apply whether $S'(x)$ is discontinuous or not.

In order to discuss the properties of $F(y)$, it is necessary to know the function $h(x)$. The expression (22) for $h(x)$ may be interpreted by the usual methods of the Heaviside calculus and calculated numerically, but in addition its behaviour for small and large values of x may be deduced from the corresponding behaviour of its representation (22) for large and small values of p, respectively. For large p, $K_1(p) \sim \pi^{1/2}e^{-p}/(2p)^{1/2}$ hence for small x, $h(x) \sim e^{p}H(x) = H(x + 1)$; for small p, $K_1(p) \sim p^{-1}$ hence for large x, $h(x) \sim (2x)^{-1/2}$. Therefore $h(x)$ is zero until $x = -1$ where it jumps to the value 1, and it ultimately tends to zero like $(2x)^{-1/2}$; the graph of $h(x)$ obtained from the numerical work is shown in Graph B, together with that of $(2x)^{-1/2}$. It is observed that $h(x)$ attains its asymptotic value very quickly, the two curves being indistinguishable for $x > 4$, and since $p^{-1}\{h(x) - (2x)^{-1/2}\} = p^{-1}\pi^{1/2}(2p)^{-1/2}\{(K_1(p))^{-1} - p\} \to 0$ as $p \to 0$, the areas under the curves are equal.

The upper limit in the integral for $F(y)$ may be replaced by $T(y)$, where $y = T - \alpha R(T)$, because $h(x) = 0$ for $x < -1$. This value T is the distance from the nose at which the characteristic $y =$ constant leaves the body surface, thus $F(y)$ depends upon the shape of the body up to this point as would be expected from the nature of supersonic flow. However, for the smooth body, expression (14) for $F(y)$ includes values of $S(t)$ only for the shorter range $0 \leq t \leq y$. Of course, this deviation from the expected range of dependence occurs in the first place in the ordinary linearized theory, and it is a remarkable result of that theory (see [3]) that although on general grounds it would be expected to introduce an error, for a *smooth* body it actually improves the accuracy. It is of interest to consider the connection between (14) and (21) further. Assuming that $S'(t)$ is continuous, it is observed that (14) is obtained from (21) by replacing the integrand in the latter by its asymptotic value $(y - t)^{-1/2}$, and replacing the upper limit $T(y)$ by y. The first step is true for the part of the range for which $t < \tau$ where $y = \tau + 4\alpha R(\tau)$ since $h(x)$ approximately attains its asymptotic form at $x = 4$; hence to obtain (14)

$$\int_\tau^T \left(\frac{2}{\alpha R(t)}\right)^{1/2} h\left(\frac{y - t}{\alpha R(t)}\right) \frac{dS'(t)}{2\pi} \tag{23}$$

is replaced by

$$\frac{1}{2\pi}\int_\tau^y \frac{S''(t)\,dt}{\sqrt{y - t}}. \tag{24}$$

For a smooth body, $S''(t)$ is continuous. Hence using the fact that the areas under the curves of $h(x)$ and $(2x)^{-1/2}$ are equal, the difference of (24) and (23) is certainly of smaller order than the error $O(\delta^3)$ in (21). (The error in (21) is a factor $1 + O(\delta)$ and for the smooth body $F(y)$ is $O(\delta^2)$.) Thus (14) and (21) are equivalent in this case and it is interesting that in fact (14) is more accurate. Near a discontinuity of $S''(t)$ it may be shown that the error in replacing (23)

by (24) is $O(\delta^{5/2})$. Hence (14) gives a poor approximation to (21) and moreover the value of $F'(y)$ given by (14) becomes infinite at the point whereas it may be shown from (21) that it should really be $O(\delta^{3/2})$; for these reasons (14) will not be used except for the smooth body. It may be remarked in connection with this that even when $S'(t)$ is discontinuous, away from the discontinuities (there must be no discontinuity of $S'(t)$ or $S''(t)$ in $\tau \leq t \leq T$) the general expression for $F(y)$ may be approximated by the Stieltjes integral

$$\frac{1}{2\pi}\int_0^y \frac{dS'(t)}{\sqrt{y-t}} \tag{25}$$

which might have been expected to provide the necessary extension of the smooth body theory to the discontinuous case.

Now a discontinuity of $S'(t)$ at $t = t_1$, say, causes a discontinuity in $F(y)$ of magnitude

$$\left(\frac{2}{\alpha R(t_1)}\right)^{1/2} \frac{\Delta S'(t_1)}{2\pi}. \tag{26}$$

Such a jump in $F(y)$ means that for the corresponding value of y, F can take a whole range of values and hence there will be a fan of characteristics $x = \alpha r - kF(y)r^{1/2} + y$ through that point on the body. If the discontinuity in slope is a decrease, $\Delta F < 0$ and the flow expands round the corner in direct analogy with the Prandtl-Meyer expansion of two dimensions; if the discontinuity in slope is an increase, the fan is reversed so that there is a fold in the flow plane and an attached shock must intervene. These occurrences are discussed in detail in Part 4 but it may be noted here that the range of slopes of the characteristics in the fan is in exact agreement with the two-dimensional result.

The behaviour of $F(y)$ for small and large y will be required in the course of the work. For y sufficiently small, there are no discontinuities of $S'(t)$ (for the bodies under consideration) and the expression (14) is applicable. Near the nose $S''(t) \doteq 2\pi\epsilon^2$ where ϵ is the initial slope $R'(0)$, i.e., the nose semi-angle, hence

$$F(y) \sim 2\epsilon^2 y^{1/2} \qquad \text{as} \qquad y \to 0. \tag{27}$$

For y sufficiently large, there will be no discontinuities near $t = y$, hence (25) may be used, i.e. $F(y) = \pi^{1/2}p^{1/2}S'(y)/2\pi = \pi^{1/2}p^{3/2}S(y)/2\pi$. The behaviour of $F(y)$ for large y is deduced from the behaviour of its operational representation, and for a body whose ultimate radius is finite, the Heaviside representation of $S(y)$ is $S(\infty) + O(p)$ for small p; therefore

$$F(y) \sim \pi^{1/2}p^{3/2}S(\infty)/2\pi = y^{-3/2}S(\infty)/4\pi \qquad \text{as} \qquad y \to \infty. \tag{28}$$

Finally, the result that $\int_0^\infty F(y)\,dy = 0$ will be required later. Since $F(y) = \pi^{1/2}p^{1/2}f(y)$, $\int_0^y F(y')\,dy' = p^{-1}F(y) = \pi^{1/2}p^{-1/2}f(y)$, and this integral tends to zero as $y \to \infty$ if $\pi^{1/2}p^{-1/2}f(y) \to 0$ as $p \to 0$. This is the case provided that the representation of f is like $p^{1/2+\beta}$, where $\beta > 0$, as $p \to 0$, i.e. $f(y) = O(y^{-1/2-\beta})$

as $y \to \infty$, a condition which is certainly satisfied for a body whose ultimate radius is finite, hence

$$\int_0^\infty F(y)\, dy = 0. \tag{29}$$

To illustrate the type of F-curve which will be encountered, the function F has been calculated for three examples of body-wake combinations, and the results are presented in Graphs C, D and E. The last one, Graph E, is the practical example of the 5–10 calibre ogival head bullet with a thinning wake, and this is taken to be the typical example. The other two are the less realistic but more simple cases of a shell with uniform wake and a body pointed at both ends (which is effectively the limiting-case of the wake narrowing to zero radius); by comparison they show the variations due to the wake. Their shapes are given by

$$\begin{aligned} R(x) &= 0.1\{1 - (1 - x)^3\}, \qquad 0 \leq x \leq 1 \\ &= 0.1, \qquad\qquad\qquad 1 < x \end{aligned} \tag{30}$$

and

$$\begin{aligned} R(x) &= 0.1(x - x^2), \qquad 0 \leq x \leq 1 \\ &= 0, \qquad\qquad\qquad 1 < x \end{aligned} \tag{31}$$

respectively, and $F(y)$ may be determined in each case from the smooth body expression (14). The curves together with the body shapes are shown in Graphs C and D. The 5–10 calibre ogival head bullet consists of a cylindrical part $ABCD$ (Figure 2), and a circular arc head drawn in the following way. The

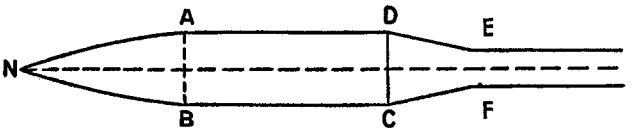

FIGURE 2

nose N is the intersection with the axis of a circle, having a radius of 5 calibres with centre 5 calibres from A on AB produced, the profile of the head is then a circular arc of radius 10 calibres through the points N and A. In this example the length of the cylindrical portion is chosen so that the thickness ratio of the bullet is 0.2. The wake is uniform after EF with its radius equal to one half that of the base, and DE is at an angle of 12° to the axis. Since there are discontinuities of slope, the general expression (21) for $F(y)$ is used, and $F(y)$ now depends on the Mach number; the calculation is for the typical value $M = 2$. The F-curve with the body shape is shown in Graph E; the characteristics are convex or concave to the oncoming stream according as $F(y)$ is positive or negative

on them, and the characteristics for which $F(y) = 0$ are straight (when r is sufficiently large for (12) to be valid) and are in the undisturbed Mach direction. It should be noted that the point $x = t$ on the body corresponds to the value $t - \alpha R(t)$ of y, hence the discontinuities in $F(y)$ occur at values of y before the corresponding values of t. The semi-angle at the nose $\approx 20°$ and this value is too large for the theory to give accurate quantitative results as will be seen in Part 4. However it was thought that it would be better to give the qualitative picture of the flow pattern for an actual practical bullet rather than just demonstrate the theory with a made up example.

4. *The Shocks*

In the two preceding sections, the appropriate solution of the equations of motion has been established but to complete the description of the flow the shocks must be determined. It is known that shocks must appear in a description of the actual flow but they are also necessary in the mathematical theory since the continuous solution breaks down in certain regions. These regions are where the characteristics run together and overlap to form a limit line, and thus the values which are given for the physical quantities cease to be unique. The breakdown is remedied by the presence of shocks which cut off the continuous solution before this occurs; the characteristics meet the shock before they meet each other. The shocks will be determined from the characteristics by the following geometrical property which is easily obtained from the shock conditions: *if two regions of supersonic flow are separated by a shock, then, to the first order in the strength, the direction of the shock bisects the Mach directions of the two regions of the flow.* (Here, the Mach direction at a point is understood to mean the outward direction making the local Mach angle with the direction of the flow at the point). This condition, though simple, is extremely powerful in the mathematical investigation and also it brings out very clearly the relation between the prediction and determination of the shocks since both are based on the running together of the characteristics.

The F-curve gives immediately a rough description of the flow pattern since it shows whether the characteristics are converging in compression ($F'(y) > 0$) when a shock will appear or diverging in expansion ($F'(y) < 0$), and of course the extreme cases of these are when F is discontinuous. For all bodies there is a shock at the front, because for small y, $F(y) \sim 2R'^2(0)y^{1/2}$ (equation (27)), and for all bodies whose radius is bounded there must be a further shock since $\int_0^\infty F(y)\,dy = 0$ (equation (29)) and $F \to 0$ as $y \to \infty$. The latter does not apply to a semi-infinite cone for example and as is known there is only the single shock attached to the vertex. The front shock is treated first since it is the simplest. It has a uniform flow on the upstream side and, in general, is a single shock since it is only not so if a subsidiary shock running into the main one is produced by a compressive protuberance near to the nose of the body; this singular occurrence is left until later.

(*i*) *The front shock.*

Although the characteristics are known and a convenient way of obtaining the shock from them is provided by the condition italicized above, success depends upon the use of the simplified form (12) instead of (10) for the characteristics. This is one of the crucial steps of the theory and for its validity requires that $\alpha r/y$ is large at all points of the shock. (This condition arose also in Part 1 in connection with the non-axisymmetrical slender body). But this is so, for at any point of the shock a characteristic specified by y behind the shock meets an undisturbed characteristic of the region ahead; these two characteristics differ in their gradients by at most $O(\delta)$ (from (9) remembering that $v = R'(x) = O(\delta)$ on the body) and they start from the axis at least a distance y apart hence, when they meet at the shock, $y/r = O(\delta)$ at very most (in actual fact it is $O(\delta^4)$). It may be remarked that the condition is also satisfied on the limit line formed as an envelope of characteristics, (this must be so since the limit line lies ahead of the shock), hence the limit line, which is of some theoretical interest, is given with y as parameter by

$$x = \alpha r - kF(y)r^{1/2} + y, \qquad kF'(y)r^{1/2} = 1. \tag{32}$$

Suppose that the shock is given by $x = \alpha r - G(r)$, then, since at the shock the disturbed characteristic behind it may be taken to be $x = \alpha r - kF(y)r^{1/2} + y$ and the undisturbed characteristic ahead is $x = \alpha r +$ constant, the "angle property" gives

$$G'(r) = \tfrac{1}{4}\, kF(y)r^{-1/2}, \tag{33}$$

and elimination of $x - \alpha r$ from the equations of the shock and the disturbed characteristic gives

$$G(r) = kF(y)r^{1/2} - y. \tag{34}$$

The two equations (33) and (34) are sufficient to specify G as a function of r, but to accomplish the solution G and r are determined separately as functions of y. First an equation for the function $r(y)$, which is the distance from the axis at which the characteristic y meets the shock, is obtained by differentiating (34) and eliminating $G'(r)$; it is

$$\frac{1}{4}\, kF(y)r^{-1/2}\frac{dr}{dy} + kF'(y)r^{1/2} - 1 = 0. \tag{35}$$

When multiplied by $F(y)$, the equation may be written as

$$\frac{d}{dy}\{\tfrac{1}{2}\, kF^2(y)r^{1/2}\} = F(y), \tag{36}$$

which on performing the integration becomes

$$r^{1/2} = \frac{2}{kF^2(y)}\int_0^y F(y')\, dy'. \tag{37}$$

The lower limit of the integral is taken to be 0 since the shock must start at the nose of the body with $y = 0$. Now (34) or (33) may be used to find G or G'; $G(r)$ gives the distance by which the shock stands ahead of the Mach cone $x = \alpha r$, and for a shock of this type it is easily found from the shock conditions that $G'(r)$ is proportional to its strength,

$$s = \frac{4\gamma}{\gamma + 1} \frac{\alpha}{M^2} G'(r) = \frac{\gamma}{\gamma + 1} \frac{\alpha}{M^2} \frac{k^2 F^3(y)}{2 \int_0^y F(y')\, dy'}, \tag{38}$$

where the strength s is defined as the ratio of the pressure jump to the undisturbed pressure.

The initial behaviour of the shock at the nose of the body may be deduced from the approximations for small y. From (27), $F(y) \sim 2\epsilon^2 y^{1/2}$ as $y \to 0$, hence the initial angle of the shock, deduced from $G'(0)$, is given by

$$\mu_0 + \frac{3}{8} \frac{(\gamma + 1)^2 M^6}{(M^2 - 1)^{3/2}} \epsilon^4, \tag{39}$$

and the initial strength by

$$\frac{3}{2} \frac{\gamma(\gamma + 1) M^6}{M^2 - 1} \epsilon^4. \tag{40}$$

For the cone, (27) is exactly true for all y; hence the shock has constant angle and strength given by (39) and (40) respectively. The results (39) and (40) for the slender cone have been found previously by Lighthill [10] and it is a check on the theory that there is exact agreement. Also, for the cone, the limit line (32) is a straight line at an angle

$$\mu_0 + \tfrac{1}{2}(\gamma + 1)^2 M^6 \epsilon^4 / (M^2 - 1)^{3/2}; \tag{41}$$

this singularity was found by Broderick [11]. The numerical solution for flow past a cone (making no assumptions of slenderness) was first carried out by Taylor and Maccoll; more complete tables have been published by the Massachusetts Institute of Technology [12]. A comparison of the theoretical predictions with these numerical results shows the limitations imposed on the theory by the assumption that the body is slender. In Graph F the value of η, the angle by which the shock angle exceeds the undisturbed Mach angle μ_0, from the tables and from the theory is plotted against M for cones of semi-angle 7.5°, 10°, and 15°. The value of γ is taken to be 1.405 since this value is used in the M.I.T. tables. It is observed that the agreement is quite good for the cone semi-angle up to 10°, the best agreement being for $M \simeq 1.5$, but that the theory becomes inaccurate after this or if M is greater than about 3.

In any practical problem the radius of the body must be bounded and the shock ultimately decays. From (37), r large on the shock corresponds to y being near to y_0, the first zero of $F(y)$ apart from $y = 0$ itself. For a body of

bounded radius, y_0 exists since $\int_0^\infty F(y)\,dy = 0$ and hence there must be at least one zero. For y near y_0 and F small, (37) becomes approximately

$$r^{1/2} \sim \frac{2}{kF^2}\int_0^{y_0} F(y)\,dy, \tag{42}$$

hence from (34)

$$G(r) \sim kF(y)r^{1/2} - y_0 \sim \left\{2k\int_0^{y_0} F(y)\,dy\right\}^{1/2} r^{1/4} - y_0\,, \tag{43}$$

and

$$s \sim \frac{\gamma}{(\gamma+1)}\frac{\alpha}{M^2}\left\{2k\int_0^{y_0} F(y)\,dy\right\}^{1/2} r^{-3/4}. \tag{44}$$

These are exactly the same results as were found in [5]; the shock stands ahead of the asymptotically straight characteristic $x = \alpha r + y_0$ by an amount $\propto r^{1/4}$ and its strength falls off like $r^{-3/4}$. For a slender body, axisymmetrical or otherwise, $G \propto l\delta(r/l)^{1/4}$ and $s \propto \delta(r/l)^{-3/4}$, where l is the length of the projectile and δ is the thickness ratio defined as (maximum cross sectional area)$^{1/2}/l$. If the body is not slender the constants in (43) and (44) are not known since F is unknown, but F depends only slightly on Mach number; hence it may be assumed that (43) and (44) still show roughly the correct dependence on Mach number. The behaviour of the shock between its initial state at the nose and this ultimate behaviour is given by (37) and (38); the distance ahead of the Mach cone increases from zero at the nose and is ultimately proportional to $r^{1/4}$, although at first the ratio of increase is *less* rapid than $r^{1/4}$.

For the slender cone the theory is now complete since, as r varies from 0 to ∞ on the shock, y also increases from 0 to ∞ and all the characteristics meet the shock, but, for a body of finite radius y varies only from 0 to y_0, i.e. only the characteristics in front of the asymptotically straight one are taken in; the characteristics behind this produce further shocks.

(*ii*) *The rear shock system.*

The simplest case is when the F-curve is of the type shown in Graph C and since it shows those basic features of the flow pattern which are common to all projectiles, without any extra complications, it will be considered first. Although the F-curve shown in the graph is for a body with a uniform wake, a similar curve may be obtained in cases of a thinning wake; however if the wake narrows too much or too rapidly the F-curve will recross the axis (see Graph E).

For this type of F-curve (Figure 3) there are two regions where the characteristics run together to form limit lines. These are the characteristics corresponding to OA and CD. From OA an attached limit line, given by (32), is formed and is subsequently replaced by an attached shock, as described in (*i*). From CD a second limit line is formed and must be replaced by a shock; this

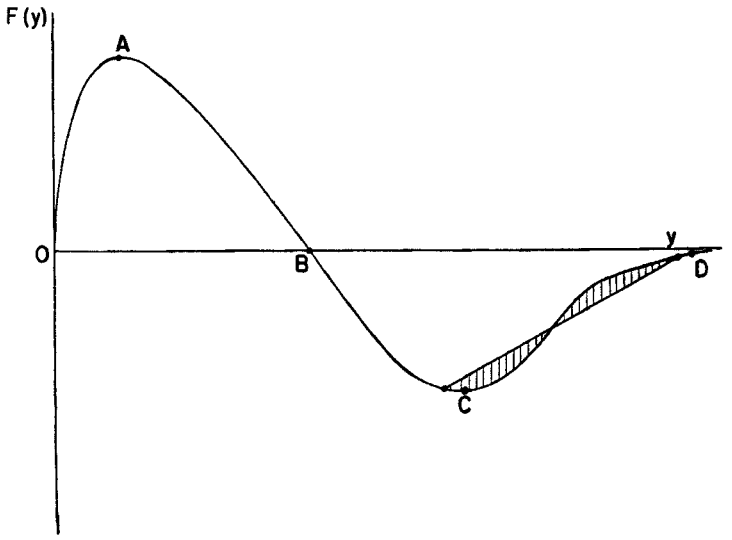

FIGURE 3

is now investigated. In the rear region, since the body is smooth, the characteristics $y = y_1$ and $y = y_2$ differ in gradient by an amount $O(\delta\{y_2 - y_1\})$ (using (9) and that u and v are continuous functions of y, of order δ) at very most, and on the body they are a distance $y_2 - y_1$ apart; hence the distance from the axis at which they intersect is large like δ^{-1}, at least. Thus for the limit line and the shock, the "$\alpha r/y$ large" approximations may be used. The limit line is then given by (32); dr/dy and dx/dy are both zero for the value of y for which $F''(y) = 0$ i.e. at the point of inflexion y_c of the F-curve; hence the limit line starts on $y = y_c$ at a large distance $\{kF'(y_c)\}^{-2}$ and it is cusped at this point. The shock replaces it in such a way that the characteristics from each side meet the shock and are cut off instead of overlapping, the geometry being governed by the angle property.

Let the equation of the shock be $x = \alpha r - G_1(r)$ and let the characteristics (equation (12)) specified by y_1 and $y_2 (y_2 > y_1)$ intersect at a point on the shock. Then the angle property requires that

$$\tfrac{1}{2}k\{F(y_1) + F(y_2)\}r^{-1/2} = 2G_1'(r), \tag{45}$$

and elimination of $x - \alpha r$ from the equations of the shock and the characteristics gives

$$G_1(r) = kF(y_1)r^{1/2} - y_1 , \tag{46}$$

$$G_1(r) = kF(y_2)r^{1/2} - y_2 . \tag{47}$$

To solve these three equations, G_1 and r are thought of as functions of either y_1 or y_2 , and the relation between y_1 and y_2 is considered. The first step is to determine this relation, which is the condition that the characteristics $y = y_1$

and $y = y_2$ meet on the shock, by eliminating G_1 and r from (45), (46) and (47). If (46) and (47) are differentiated with respect to r and added, and then the term $2G_1'(r)$ is replaced by (45), the equation

$$\{kF'(y_1)r^{1/2} - 1\}\, dy_1 + \{kF'(y_2)r^{1/2} - 1\}\, dy_2 = 0, \tag{48}$$

is obtained. But r is known in terms of y_1 , y_2 from the difference of (46) and (47), hence

$$\{F(y_2) - F(y_1) - (y_2 - y_1)F'(y_1)\}\, dy_1 + \{F(y_2) - F(y_1) - (y_2 - y_1)F'(y_2)\}\, dy_2 = 0. \tag{49}$$

With some manipulation, this can be put in a form which can be integrated:

$$F(y_2)\, dy_2 - F(y_1)\, dy_1 = \tfrac{1}{2}d\{(y_2 - y_1)[F(y_2) + F(y_1)]\}, \tag{50}$$

whence

$$\int_{y_1}^{y_2} F(y)\, dy = \tfrac{1}{2}(y_2 - y_1)\{F(y_2) + F(y_1)\}, \tag{51}$$

the constant of integration being put equal to zero since $y_2 = y_1$ must be a solution. Coupled with the expression for r which is

$$\frac{1}{kr^{1/2}} = \frac{F(y_2) - F(y_1)}{y_2 - y_1}, \tag{52}$$

the shock is determined; G_1 or G_1' may be obtained from either of (45), (46) and (47).

The results (51), (52) for the shock are already neat mathematically though at first sight the process of relating y_1 and y_2 might appear tiresome. But they assume an even more stimulating form when their interpretation with respect to the F-curve is considered. For, the left hand side of (51) is the area whose four sides are the ordinates $y = y_1$ and $y = y_2$, the axis and the curve, whilst the right hand side is the trapezoidal area between the same ordinates, the axis and the straight segment joining the points y_1 and y_2 of the curve. Hence the condition (51) states that *the "lobes" cut off on each side of the curve by this segment must be equal in area.* Moreover, from (52), the *gradient of this segment is equal to* $(kr^{1/2})^{-1}$. A typical segment with the lobes shaded is shown in Figure 3.

Now the path of the shock may be traced by considering the whole series of segments; typical ones 11′, 22′, 33′, $\cdots$ are represented in Figure 4. Clearly the limiting segment for which the lobe area has decreased to zero is the tangent to the curve at the point of inflexion $y = y_e$; it is shown in the sketch as 11′, and since it has the largest gradient it corresponds to the point on the shock nearest to the body. Here, the shock starts with zero strength (since $F(y)$ is continuous at $y = y_e$) and, as it must by the method of determination, it starts at the same point as the limit line. The gradients of the successive segments then decrease, corresponding to increasing r, tending ultimately to be horizontal

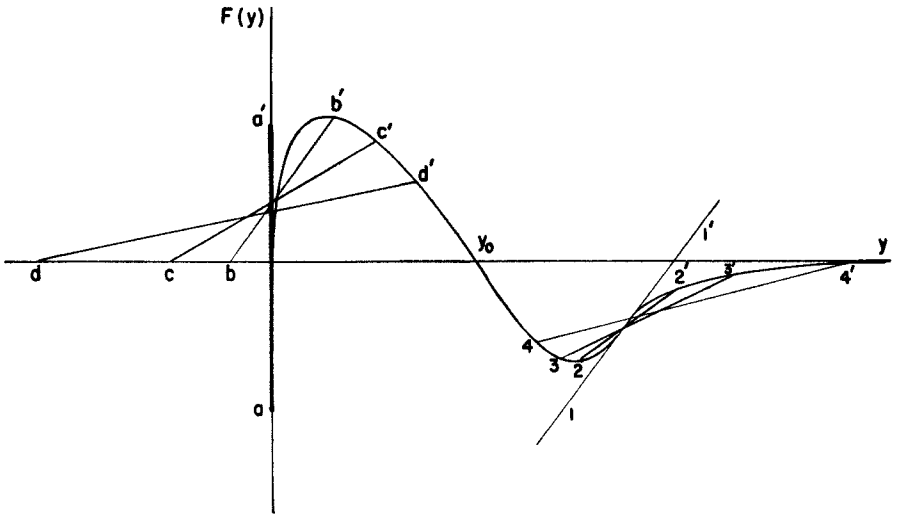

FIGURE 4

as $y_2 \to \infty$ and $y_1 \to y_0+$, the zero of $F(y)$. The strength of the shock at any point is $\gamma M^2\{F(y_2) - F(y_1)\}(2\alpha r)^{-1/2}$ (see (67) below); as r increases, the shock first increases in strength and then decays. To study the decay at large distances, the approximations y_2 large, $y_1 - y_0$ small may be used, hence (51) may be approximated as

$$\int_{y_0}^{\infty} F(y)\,dy = \tfrac{1}{2}(y_2 - y_1)(y_1 - y_0)F'(y_0), \tag{53}$$

since $F(y) = O(y^{-3/2})$ as $y \to \infty$, and (52) as

$$kr^{1/2} = -\frac{y_2 - y_1}{(y_1 - y_0)F'(y_0)} = -\frac{2\int_{y_0}^{\infty} F(y)\,dy}{(y_1 - y_0)^2 F'^2(y_0)}. \tag{54}$$

Then, from (46) $G_1 = k(y_1 - y_0)F'(y_0)r^{1/2} - y_0$, and from (54) $y_1 - y_0$ is known in terms of r, hence

$$G_1 = -\left\{-2k\int_{y_0}^{\infty} F(y)\,dy\right\}^{1/2} r^{1/4} - y_0\,. \tag{55}$$

It was found, see (43), that, at large distances, the front shock was a distance $\{2k\int_0^{y_0} F(y)\,dy\}^{1/2}r^{1/4}$ ahead of the straight characteristic $x = \alpha r + y_0$ and now the rear shock is found to be $\{-2k\int_{y_0}^{\infty} F(y)\,dy\}^{1/2}r^{1/4}$ behind. In the previous paper, [5], these results were found but the constants in the expressions were the same. This led the author to the result deduced in Part 3 that, in fact, $\int_0^{\infty} F(y)\,dy = 0$ which proves the equality.

Du Mond, Cohen, Panofsky and Deeds [13] have obtained numerical results from experiments on the flight of bullets. They verify that if r is greater than about 1,000 projectile diameters the distance between the two shocks is propor-

tional to $r^{1/4}$ and the strengths fall off as $r^{-3/4}$. They also find that the front and rear shocks balance (i.e. they are equal distances from the straight characteristic) for r greater than only about 100 projectile diameters. However, if the above asymptotic expressions for large r are extended to include the next most important term it is found that the shocks are

$$x - \alpha r = y_0 \mp \left\{2k \int_0^{y_0} F(y)\, dy\right\}^{1/2} \left(r^{1/4} + \frac{r^{-1/4}}{2kF'(y_0)}\right), \tag{56}$$

respectively, which indicates that the balance will be obtained before the $r^{1/4}$ law operates. At these smaller distances, the experimental values of n, where the strength $s \propto r^{-n}$, were found to be approximately between 0.85 and 0.90 as opposed to the ultimate value of 0.75.

It would be expected that the more general procedure adopted for the rear shock could be applied to the front one, and indeed this is true. If the F-curve is extended to include the y-axis for $y < 0$, where the characteristics are the straight lines $x = \alpha r + y$, $y =$ constant, segments cutting off lobes of equal area determine the shock, and the slope of the segment is again $(kr^{1/2})^{-1}$. Such segments are shown as aa', bb', cc', $\cdots$ in Figure 4; the limiting one is the tangent to the curve at the origin and, since it is vertical it implies that $r = 0$ i.e. the shock is attached to the nose. The distance from the axis increases as the segment gradients decrease, and as $r \to \infty$, the segments tend to the horizontal, in this case $y_1 \to -\infty$ and $y_2 \to y_0 -$. Thus Figure 4 gives a very simple interpre-

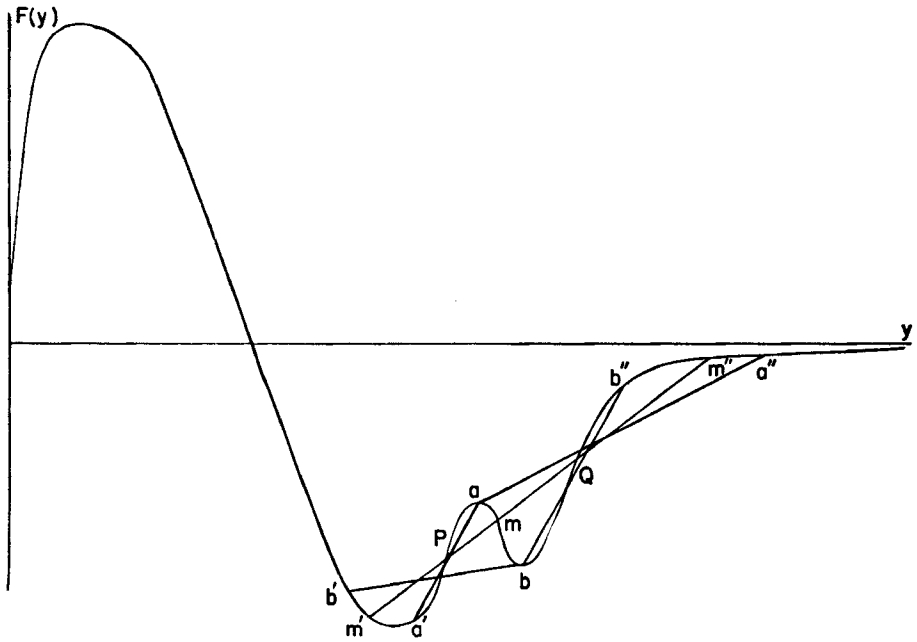

FIGURE 5

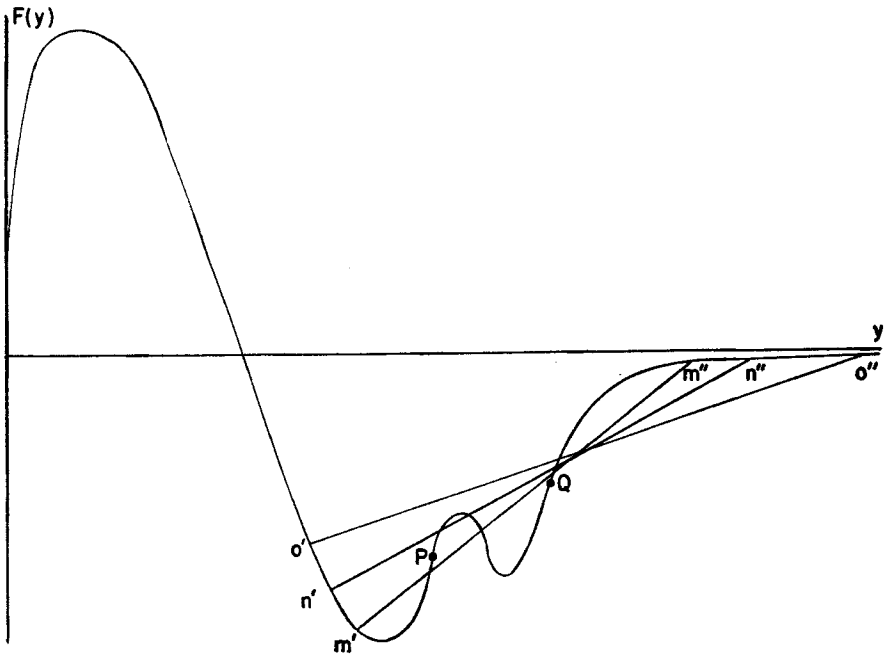

FIGURE 6

tation of the flow pattern. The characteristics $0 < y < y_c$ lie between the shocks (as before, y_c is the value of y at the point of inflexion of $F(y)$), those for which $0 < y < y_0$ meeting the front one and $y_0 < y < y_c$ the rear one, the asymptotically straight characteristic y_0 alone reaching infinity. The "segments" and "angle property" give a clear account of the progress of the shocks to infinity.

Possible complications to this fundamental F-curve will now be considered. Suppose that due to some corrugation in the body surface there is a "kink" in the F-curve. There are two possible cases and first that of a "sharp kink" is considered; this case is shown in Figure 5 and the meaning will become apparent in the discussion. There are now two points of inflexion, P and Q, at which $F'(y)$ is positive and hence shocks start from these two points. The question is: what is their subsequent behaviour? At first, in the neighbourhoods of P and Q, respectively, small segments can be drawn for the development of each shock, but later these will interfere with each other. To see what happens then, consider the following argument: Take points a and b in opposite extreme positions as shown and draw the equal area segments of each set, aa', bb', and aa'', bb''. The segmental broken-lines $a'aa''$ and $b'bb''$ are bent in opposite directions, therefore by continuity there exists a point m between a and b such that the corresponding segmental line $m'mm''$ comprises a single straight line. In a sense, the characteristics corresponding to points such as a, b and m which lie between P and Q meet both shocks since segments belonging to each can be drawn, but this must be interpreted as meaning that after meeting its first shock,

the characteristic would, if continued, meet the second one; but of course in reality it is cut off at the first. However for m since mm' and mm'' have the same gradient, this characteristic meets both shocks at the same distance from the axis and therefore at the *same point*, thus at this point the two shocks join and only a single shock proceeds beyond. The whole behaviour is described as follows: Shocks start at points P and Q with the segments occupying the limiting positions of tangents to the curve, and their initial progress as r increases is described by the segments decreasing in gradient through typical positions $a'a$ and bb'', respectively, to the positions $m'm$ and mm''. At this point the shocks join, and so far all the characteristics between m' and m'' have been included. Then a single shock proceeds described by single segments whose end points decrease from m' and increase from m'', the intermediate intersections with the curve being ignored since these characteristics have already been cut off by the shocks; however the separate sums of the lobe areas on each side of the segment must still be equal. This second stage is shown in Figure 6. The shock now goes to infinity just as in the original case, Figure 4, since the kink plays no further part in the development; as $r \to \infty$, the segments tend to the horizontal with $y_1 \to y_0+$ and $y_2 \to \infty$. Finally in Figure 7 the flow plane is shown, with the

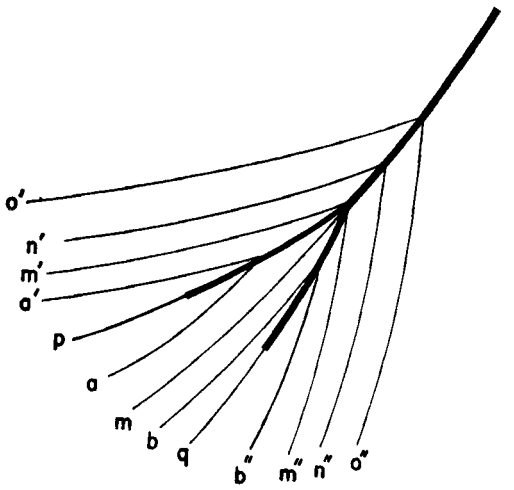

FIGURE 7

characteristics lettered corresponding to their representative points on the F-curve. It is clear from the angle property, that the two shocks meet at a finite angle (they do not just coalesce) and the single shock which continues from the point of intersection starts in a direction strictly between the two incident shocks.

The second case, that of a "flat kink," can be dealt with very briefly. In this case, see Figure 8, no points a and b can be found between P and Q such that the segmental lines are bent in opposite directions; they are all concave to the axis. This means that the segments coming round from Q are always

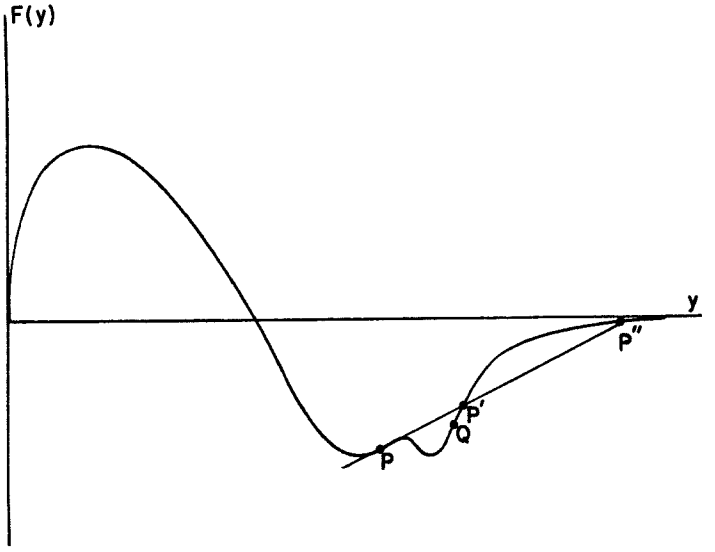

FIGURE 8

steeper than even the tangent at P, hence the shock originating at Q takes in all the characteristics near P and cuts them off before they can run together to form a shock of their own. There is just a single shock in this case. Clearly the criterion is that the shock does or does not appear according as the area of the lobe $P'P''$ is smaller or greater than the area of the lobe PP', where the tangent at P meets the curve again in P' and P''. It may be remarked that if the "kink" occurs in the part of the F-curve before y_0 , a subsidiary shock may run into the front shock and the more simple theory given earlier in (i) will require modification.

The question of kinks has been gone into in considerable detail because it highlights all the points in the use of the F-curve; any F-curve can now be interpreted by this technique. It is necessary, however, to say more about the case in which F has discontinuities. For, suppose as in Figure 9 there is a compressive discontinuity of $F(y)$; then segments may be drawn in the usual way,

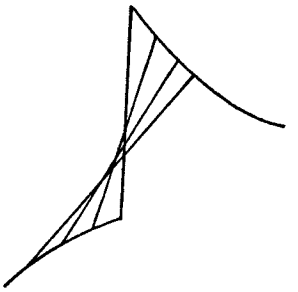

FIGURE 9

but the limiting one, showing where the shock starts, has infinite gradient since it lies along the discontinuity itself. According to this the shock starts at $r = 0$. The shock is attached to the body as expected, but it starts inside the body even and thus is not quite in the correct position. There is no difficulty in interpreting the F-curve, but its use to describe the flow depends on the approximation $\alpha r/y$ large being valid and this is not true near the body on an attached shock; some justification or modification is required. At large distances the theory is all right and the only difficulty is the initial behaviour near the body. Now, consider the discontinuity in the body slope to be superimposed on an already existing smooth body so that in the mathematical theory terms must be added on to the smooth body solution to take account of this additional discontinuity. In fact, suppose that for the smooth body the $f(x)$ of Part 2 is $f_0(x)$ and that the additional term added on to $f_0(x)$ at the discontinuity $x = x_1$, $R(x) = R_1$ is $f_1(x)$. Then (10) becomes

$$x = \alpha r - c_0(y, r) - c_1(y, r) + y, \tag{57}$$

where $c_0(y, r)$ and $c_1(y, r)$ denote $c(y, r)$ with $f(x)$ replaced by $f_0(x)$ and $f_1(x)$ respectively; the integrals in $c_1(y, r)$ have the lower limit $\bar{y} = x_1 - \alpha R_1$, the value of y on the characteristic through the discontinuity. It is clear that on the shock $\alpha(r - R_1)/(y - \bar{y})$ is large (in the same way as $\alpha r/y$ is large on the front shock); hence from (10) it is approximately true that

$$c_1(y, r) = kF_1(y)(r^{1/2} - R_1^{1/2}), \tag{58}$$

where $F_1(y)$ represents the contribution to $F(y)$ of f_1. Near the body, since the deviation of y from $\bar{y}$ is relatively small, $c_0(y, r)$ may be approximated as $c_0(\bar{y}, r)$, and at large distances by $kF_0(y)r^{1/2}$, hence it is taken to be

$$C(r) + kF_0(y)(r^{1/2} - R_1^{1/2})$$

everywhere, where $C(r) = c_0(\bar{y}, r) - kF_0(\bar{y})(r^{1/2} - R_1^{1/2})$. Hence, for an attached rear shock, the characteristics may be taken to be

$$x = \alpha r - kF(y)(r^{1/2} - R_1^{1/2}) - C(r) + y, \tag{59}$$

where $F(y) = F_0(y) + F_1(y)$, and $C(r)$ is a function of r alone, being the correction for the deviation near to the body of the characteristic from its large distance value; $C(r)$ and $R_1^{1/2}$ are of course negligible at large distances. Use of (59) involves only very slight modifications to the determination of the shock; the characteristics and shock equations all have an additional term $C(r)$, and $r^{1/2}$ is replaced everywhere by $r^{1/2} - R_1^{1/2}$. The results become

$$\int_{y_1}^{y_2} F(y)\, dy = \tfrac{1}{2}(y_2 - y_1)\{F(y_2) + F(y_1)\}, \tag{60}$$

$$\frac{1}{k(r^{1/2} - R_1^{1/2})} = \frac{F(y_2) - F(y_1)}{y_2 - y_1}, \tag{61}$$

$$G_1(r) = kF(y_1)(r^{1/2} - R_1^{1/2}) + C(r) - y_1 \,. \tag{62}$$

Hence the F-curve may be interpreted exactly as before with the slight change that the gradients of the segments give the values of $\{k(r^{1/2} - R_1^{1/2})\}^{-1}$. This is an improvement since the shock now starts at $r = R_1$ as it should instead of at $r = 0$. Essentially the modification is to use a procedure similar to that for the front shock where the characteristics from the pointed body shape were superimposed on the previously undisturbed motion. In the above, the characteristics which form the shock are superimposed on a motion which is already disturbed, but the solution is the same since near the body those characteristics which already exist can be assumed to be similar in shape (this corresponds to putting $y = \bar{y}$ in c_0), the variation of y being small, and since for the superimposed characteristics the large distance approximation may be used.

If the discontinuity is expansive there will be a fan of characteristics leaving the point. The range of values of dx/dr in the fan will be, from (59), $-\frac{1}{2}k\ \Delta F \cdot R_1^{-1/2}$ and from (26), $\Delta F = 2^{1/2}\alpha^{-1/2}R_1^{1/2}\ \Delta R'$, hence the range is $\frac{1}{2}(\gamma+1)M^4(M^2-1)^{-1} \times$ the angle turned through by the stream $(-\Delta R')$. The result is in exact agreement with the two dimensional Prandtl-Meyer expansion to this order of approximation; this is because any local change of motion on the surface of the body is two dimensional in its nature, since there the radius of the body is large compared with the infinitesimal distance in which the corner is turned. The agreement provides further support for the theory.

5. *Examples. The 5-10 Calibre Ogival Head Bullet*

In this section, the technique established in Part 4 is applied to special body shapes and in particular to the practical example of the ogival head bullet. Graphs C, D and E show the calculated values of $F(y)$ for three different shapes, the details of which have been given in Part 3. The first two are the extreme cases of a uniform wake and of no wake at all, and the body in Graph E has a typical wake between these two extremes. The F-curve of Graph C is the simple one which gives the basic flow pattern already described in detail in Part 4, and it is unnecessary to say more. The parabolic profile of Graph D is typical of bodies pointed at both ends, but it is an ideal case without physical reality since in practice the boundary layer would break away towards the rear and produce a narrow wake. However, it is of interest as the limiting case of no wake at all. The F-curve of Graph D can be interpreted quite easily; there is the usual attached shock at the front but rather surprisingly the shock at the rear is detached, starting on the characteristic from the tail with its start corresponding to the non-vertical tangent at $y = 1-$. (Note, the tangent at $y = 1+$ is vertical but since $F'(1+) < 0$, this can never be the limiting position of one of the segments). For the actual flow the F-curve would be smoothed out at $y = 1$ into a region of high curvature.

The F-curve of Graph D is singular in any case because it tends to 0 through

positive values as $y \to \infty$, whereas for any actual flow there must be a wake and therefore $F \to 0-$ as $y \to \infty$. But, by comparison with Graph C, it shows that the narrowing of the wake tends to make the F-curve recross the axis; this also occurs in Graph E. The possibility of further zeros of $F(y)$ raises the important question of whether more than two shocks continue to infinity. It is clear from the foregoing arguments that the only characteristics which can reach infinity without first meeting a shock are those for which y is a zero of $F(y)$ at which $F'(y) < 0$; for, to avoid meeting a shock formed by other characteristics such a shock must be asymptotically straight, and if $F'(y) > 0$ it is a member of a limit line and predicts the presence of a shock to cut it off! Thus when there is just a single "expansive" zero there are ultimately only two shocks, but if F recrosses the axis (as in Graph E) the possibility of more shocks must be considered. Suppose that F is of the form shown in Figure 10 so that there are

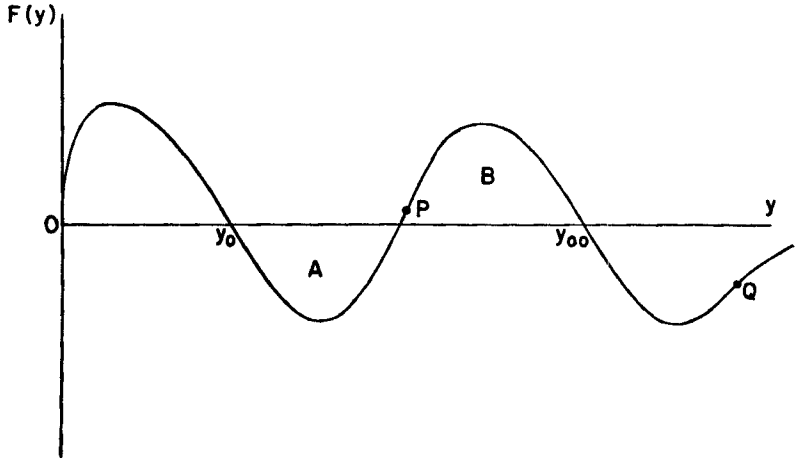

FIGURE 10

two expansive zeros y_0 and y_{00}. Then shocks start at O, P and Q and their development is described by the usual segments. If two of the sets of segments clash, then, as in the discussion of kinks in Part 4, the corresponding shocks join (or possibly one of them is not formed), hence for the three shocks to reach infinity without this occurring, the equal area segments must tend to the positions $(-\infty, y_0-)$, $(y_0+, y_{00}-)$, $(y_{00}+, +\infty)$ respectively as $r \to \infty$. For this to be possible, area A must be equal to area B. If area $B >$ area A the middle shock runs into the front one and the whole of the curve between 0 and y_{00} should be considered as the front part of the F-curve, $y = y_{00}$ being the dividing characteristic which appears in (42) and (43); the portion A is treated just as a kink in the front part $0 < y < y_{00}$ of the curve. If area $B <$ area A, the middle shock joins with the rear one and the portion B is treated as a kink in the rear part $y_0 < y$ of the curve. The condition area A = area B is very unlikely to be satisfied unless specially imposed, hence although it is possible for three shocks to reach infinity, in general since two physical quantities can never be exactly equal it

may be concluded that there will be only two shocks at sufficiently large distances. However in other analogous problems such as the periodic oscillation of a piston in a tube, this type of condition may well be satisfied closely enough and the methods of this paper may be applied for the asymptotic form of the shock, etc., (see Appendix) but it is not important for the present problem so the details are not given here.

The ogival head bullet has been described in Part 3. The Mach number is taken to be 2 and, for this value, photographs show that the ratio of the ultimate wake diameter to the base diameter is about $\frac{1}{2}$, and a typical value for the angle turned through at the base is 12°. To approximate this the wake diameter is taken to decrease linearly, with the boundary at 12° to the axis, from the base to half its value, after which it continues to infinity downstream with constant value. The compressive discontinuity in the wake boundary would in fact be smoothed out as a region of very high curvature but it is most easily approximated by the discontinuity, and it is of interest to study an example with an attached rear shock. In any case the only difference would be that the jump in the F-curve would be smoothed out into a region of extremely rapid increase in F, implying that the shock started very close to the body. For large y, $F(y) \sim -S(\infty)/(4\pi y^{3/2})$ (see equation (28)), hence the F-curve ultimately tends to the axis from below; this is not shown in Graph E since it does not extend to sufficiently large values of y. Figure 11 shows the full curve; in order to include all the features it is not drawn in correct proportion. There are two expansion

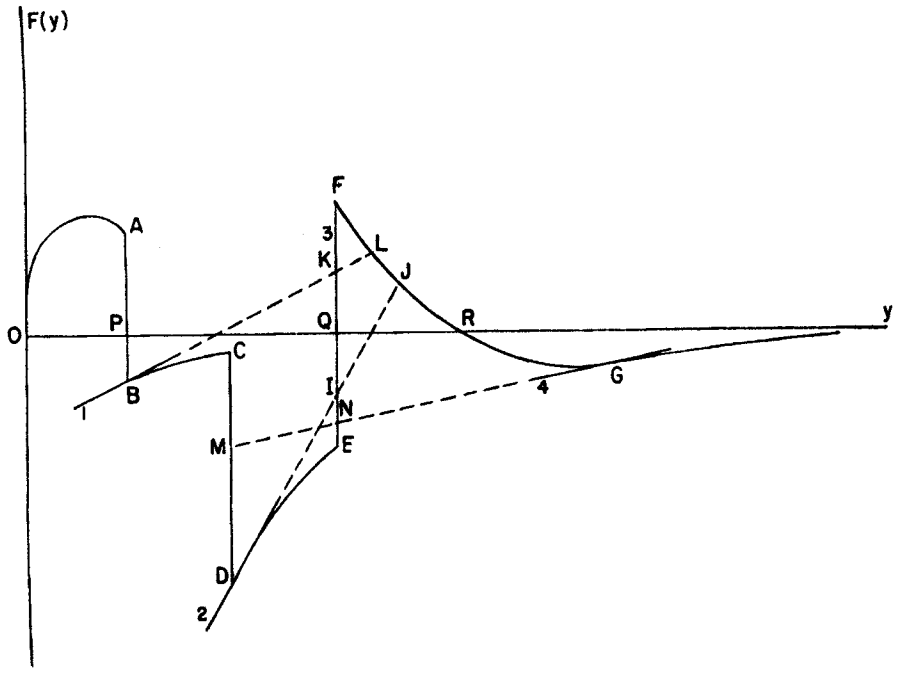

FIGURE 11

fans of characteristics from the discontinuities AB and CD, and a "reversed" fan, which will be replaced by an attached shock, from the compressive discontinuity EF. The front shock is of the usual type and can be treated quite straightforwardly; since area $PBCDEQ >$ area QFR, there are no subsidiary shocks running into it. The asymptotically straight characteristic corresponding to P which separates the characteristics of the front and rear shocks, is in this case a member of the first expansion fan. Behind this characteristic there are four regions for which "equal area segments" can be drawn; the limiting positions are the tangents numbered 1 to 4 in the sketch. Thus there is a possibility of 4 shocks being formed but they do not necessarily materialize since the characteristics of any one may meet another shock first as was the case for a "flat kink" in Part 4. The first two S_1 and S_2 , as shown by the segments 1 and 2 form on the last characteristics of the expansion fans, S_3 is attached (the limiting segment 3 lying along the discontinuity itself), and S_4 is formed by the final recompression to zero. There is no question that S_3 actually appears; since it is attached it obviously does. To determine whether S_2 appears, 2 is continued to meet the curve again in I and J. If area $FJI >$ area DEI, the equal area segment belonging to S_3 and passing through D is greater in slope than 2, hence S_2 does not form since the characteristics are taken in by S_3 before this happens. From Graph E, this is found to be the case hence S_2 does not appear. Similar arguments may be applied to S_1 and S_4 . It is found that S_1 is formed, since area $BCDEK >$ area KFL, and it ultimately joins with S_3 as in the case of the "sharp kink." For S_4 , it depends on whether area $MDN <$ area NFG or not, the former corresponding to shock formation. It is difficult to decide this without much computational work but it is not very important in the flow pattern since the shock would be extremely weak. Ultimately of course there are just two shocks; the segments (y_1 , y_2) for the front shock have $y_1 \to -\infty$, $y_2 \to y_0-$ and for the rear one $y_1 \to y_0+$, $y_2 \to +\infty$. The ultimate decay of the shocks is the same for all bodies and has been described in Part 4. The drawing of the equal area segments has been done very roughly and the resulting flow pattern is shown in Graph G. Unfortunately it is impossible to show the subsidiary shocks running into the main one since they are formed at such large distances.

The appearance of shocks starting on the final characteristics of the two expansion fans in this specific example raises the question of whether this is always the case (provided no other shock intrudes) and whether an expression, in terms of the body shape at the discontinuity, for the distance at which a shock forms may be obtained. The answers to these questions depend upon the behaviour of the F-curve; a shock is formed on the last characteristics of an expansion if $F'(\bar{y}+) > 0$, $F''(\bar{y}+) < 0$, and the distance from the axis at which it starts is given by $r = \{kF'(\bar{y}+)\}^{-2}$, where $\bar{y}$ is the value of y at which the discontinuity occurs. If $R'(t)$ is discontinuous at $t = t_1$ by an amount $\Delta R' < 0$, and $R(t_1) = R_1$ then the largest term in the expression (21) for $F(y)$ is

$$\sqrt{\frac{2R_1}{\alpha}}\, h\left(\frac{y - t_1}{\alpha R_1}\right)\Delta R', \tag{63}$$

and its contribution to $F'(y)$ is

$$\sqrt{\frac{2}{\alpha^3 R_1}}\, h'\left(\frac{y - t_1}{\alpha R_1}\right)\Delta R'. \tag{64}$$

Since $\Delta R' < 0$ and $h'(x)$ is negative and increases for increasing x, it is seen that the shock does form on the final characteristic of an expansion fan, and the estimate provided by (64) for the distance r_s at which it is formed is given by

$$\left(\frac{r_s}{R_1}\right)^{1/2} = \frac{(M^2 - 1)^{3/2}}{(\gamma + 1)M^4\, \Delta R'\, h'(-1)}, \tag{65}$$

and $h'(-1) \simeq -0.4$. Thus r_s/R_1 depends only on the angle turned through and the Mach number. A more accurate expression will be obtained by using the full expression for $F(y)$; then other smaller terms, involving the curvature of the body surface after the expansion, will be included. The values of r_s given by (63) and the actual F-curve, for the first expansion fan of the ogival head bullet, are .814 and 6.53 respectively. The approximation (65) is very bad in this case since the body is not slender enough for $\delta^{1/2}$ to be really small.

All possible F-curves have not been considered but the work of Parts 4 and 5 includes most of the important features, and gives sufficient explanation for the use of the technique in any given problem.

6. *The Pressure Signature*

In these final two Parts, 6 and 7, some physical properties of the flow, whose geometry has been established in the preceding sections, will be considered. From Bernoulli's equation, which is approximately true since the small entropy changes at a shock contribute a term of smaller order,

$$\frac{p}{p_0} = -\gamma M^2\left\{u + \tfrac{1}{2}(u^2 + v^2)\right\}, \tag{66}$$

where p is the pressure in excess of the undisturbed pressure p_0.

The values of u and v are given in Part 2 in terms of the arbitrary function $f(x)$ which is determined by the methods of Part 3. On the body surface and in regions near to the body but away from the shocks, the theory just reproduces the linearized results and it is therefore unnecessary to recapitulate them here; however, on the shocks and at large distances (which are closely connected since in a sense the points of a shock are "effectively at large distances") the theory gives values which are unobtainable or incorrect in the linearized theory, hence they are set out here.

At a shock the jump in u is $-\{F(y_2) - F(y_1)\}/(2\alpha r)^{1/2}$ as is explained below, hence the pressure jump is given by

$$\frac{\Delta p}{p_0} = \frac{\gamma M^2}{\sqrt{2\alpha}}\,\frac{F(y_2) - F(y_1)}{r^{1/2}}, \tag{67}$$

where y_1 and y_2 are the values of y on the characteristics on each side. For the front shock, $F(y_1) = 0$, the value of u ahead is 0 and behind the shock the approximation $\alpha r/y$ large may be used for u, hence (67) follows. For an *attached* rear shock, arguments similar to those used in Part 4 to determine the shock are required; the *jump* of pressure is due to the "superimposed discontinuity" and for this part of the disturbance the points of the shock are effectively at a large distance (see p. 326). Thus the jump in u near the body is $-F_1(y_2)/(2\alpha r)^{1/2}$, and $F_1(y_2) = F(y_2) - F_0(y_2) \doteq F(y_2) - F_0(y_1) = F(y_2) - F(y_1)$ (using that $y_2 - y_1$ is small and $F_0(y)$ is continuous), thus (67) is correct near the body; it is also correct at large distances of course and hence may be used everywhere. The pressure jump at the front shock has been discussed in detail in Part 4. An attached rear shock starts at the body with

$$\frac{\Delta p}{p_0} = \frac{\gamma M^2}{\sqrt{2\alpha}} \frac{\Delta F}{R_1^{1/2}} = \frac{\gamma M^2}{\alpha} \Delta R', \tag{68}$$

which is in agreement with the two dimensional case, and decays at infinity as described below.

When the distance from the body is sufficiently large for the approximation $\alpha r/y$ large to be used irrespectively of whether the point is on a shock or not, the expression for p becomes, to a first approximation,

$$\frac{p}{p_0} = \frac{\gamma M^2}{\sqrt{2\alpha}} \frac{F(y)}{r^{1/2}}, \tag{69}$$

where y is determined from

$$x = \alpha r - kF(y)r^{1/2} + y. \tag{70}$$

Discontinuities in p will occur as shocks are crossed since the value of y, specifying the characteristic on which the point (x, r) lies, will change discontinuously; the result is, of course, in agreement with (67). At very large distances, there are just two shocks (in general) for all projectile shapes; between the shocks y is near y_0, a certain zero of $F(y)$, and behind the rear shock y is large. Hence, between the shocks, (69) becomes, using (70),

$$\frac{p}{p_0} = \frac{\gamma M^2}{\sqrt{2\alpha}} \frac{\alpha r - x + y_0}{kr}. \tag{71}$$

Thus at a fixed large distance r, the pressure falls *linearly* between the shocks at a rate $\gamma(\gamma + 1)^{-1}\alpha M^{-2} r^{-1}$ per unit distance and *the rate of fall is independent of the body shape.* (Since $F(y)$ does not appear in formula (71) it will be true for non-slender bodies). The result assumes a simpler form in a frame of reference such that the fluid ahead of the projectile is at rest; then the rate of fall of pressure becomes (for $\gamma = 1.4$ and $a_0 = 340$ metres/sec)

$$0.2\left(1 - \frac{1}{M^2}\right)^{1/2} r^{-1} \quad \text{atmospheres/millisecond}, \tag{72}$$

where r is measured in metres. If the projectile is well supersonic, the factor depending on Mach number is approximately unity so that if a suitable measuring instrument were used, (72) would give a simple estimate of the miss-distance r of a supersonic projectile from the observation point. Behind the rear shock $F(y) \sim -y^{-3/2}S(\infty)/4\pi$, hence

$$\frac{p}{p_0} = -\frac{\gamma M^2}{4\pi\sqrt{2\alpha}} \frac{S(\infty)}{r^{1/2}(x - \alpha r)^{3/2}}, \tag{73}$$

and at the shock where $x - \alpha r = \{2k \int_0^{y_0} F(y)\, dy\}^{1/2} r^{1/4}$, the value is

$$-2^{7/8}\gamma(\gamma + 1)^{-3/4}M^{-1}(M^2 - 1)^{5/16}\left\{\int_0^{y_0} F(y)\, dy\right\}^{-3/4} (S(\infty)/4\pi)r^{-7/8}. \tag{74}$$

Summing up then, at very large distances, the pressure at the front shock is

$$2^{1/4}\gamma(\gamma + 1)^{-1/2}(M^2 - 1)^{1/8}\left\{\int_0^{y_0} F(y)\, dy\right\}^{1/2} r^{-3/4} \quad \text{atmospheres}, \tag{75}$$

it falls linearly at a rate $\gamma(\gamma + 1)^{-1}M^{-2}(M^2 - 1)^{1/2}r^{-1}$ atmospheres per unit distance to minus this value at the rear shock where it jumps to the value given by (74) and finally returns to zero as shown by (73).

The pressure signature in the intermediate positions, before the final "N-wave" is attained, is of the same type of curve as the F-curve but, as r increases, it is stretched out as the characteristics diverge, the amplitude falls off due to

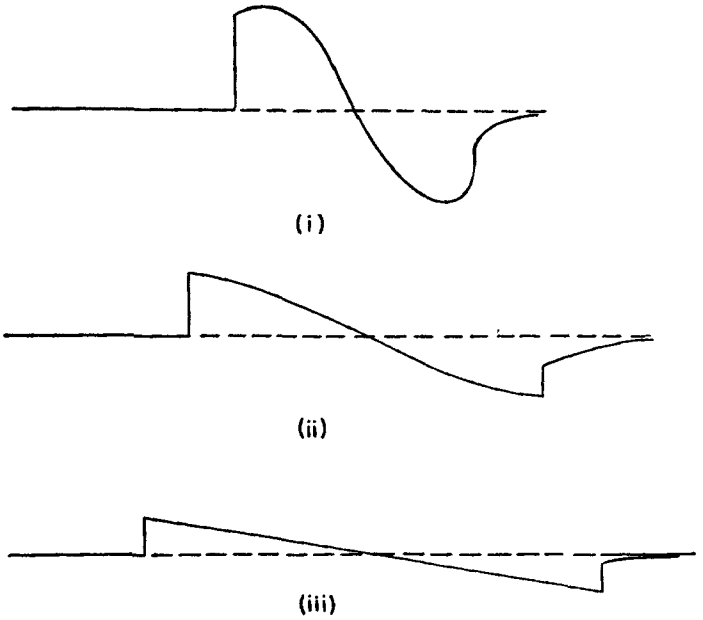

FIGURE 12

the factor $r^{-1/2}$, and sections of the curve are cut out where there are shocks. For the basic problem of Part 4 which has an F-curve as shown in Figure 3, successive stages would be roughly as in Figure 12: (i) is just before the rear shock is formed, (ii) an intermediate position with both shocks and (iii) the final N-wave.

7. *The Drag and Mass Outflow*

The drag on a body can be found in two ways; directly from the pressure forces acting on the body, and indirectly from the rate at which energy or longitudinal momentum is transported across a "control surface" enclosing the body. In the linearized theory only the first method is appropriate since the theory is incorrect away from the body. However, the theory established in this paper gives an accurate first approximation everywhere, hence either method could be used. The theory reproduces linear theory near and on the body; therefore the direct method gives nothing new, but it is of considerable interest to carry out a check by means of the indirect one.

With the frame of reference such that the undisturbed fluid is at rest, the control surface Σ is taken to be a plane Π perpendicular to the direction of motion, extending beyond the disturbed region and moving with the body; the surface may be completed in the undisturbed fluid in any way. In this frame of reference the velocities of the fluid particles are Uu, Uv and the rate at which matter crosses Π is $\rho U(1 + u)$, where ρ is the density. The rate at which work is done on the fluid DU, where D is the drag, is equal to the rate of gain of total energy

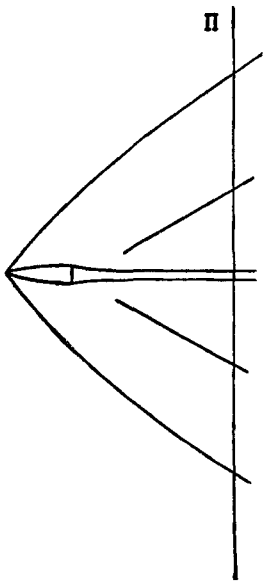

FIGURE 13

(kinetic and internal) of the fluid in Σ, minus the rate of work done by the pressures acting at Π. Hence letting Π become of infinite radius

$$(76) \qquad DU = \int_0^\infty [(p_0 + p)Uu + \rho U(1 + u)\{e - e_0 + \tfrac{1}{2} U^2(u^2 + v^2)\}]2\pi r \, dr,$$

where the suffix 0 refers to the undisturbed values and e is the internal energy per unit mass. By continuity, the mass flux through Σ must be 0, hence

$$(77) \qquad \int_0^\infty \{\rho U(1 + u) - \rho_0 U\}2\pi r \, dr = 0,$$

and thus (76) can be written as

$$(78) \quad D = \int_0^\infty \left[pu + \rho(1 + u)\left\{ e - e_0 + p_0\left(\frac{1}{\rho} - \frac{1}{\rho_0}\right) + \tfrac{1}{2} U^2(u^2 + v^2) \right\} \right] 2\pi r \, dr.$$

This is the form in which the drag, instead of being related to the flux of total energy, is related to the flux of "wave energy" which ignores that part of the internal energy associated with compression by the undisturbed pressure p_0, and it is proportional to the square of the amplitude and to the wave length. Continuity requires that the total mass flux should be zero but it is important to check that this is true in this theory. Since x is known simply as a function of y and r, the flux is most easily determined by considering the outflow through a large cylinder co-axial with the projectile. It is, to the first order, $\int \rho_0 U v 2\pi r \, dx$ where r is constant in the integration, and this by (11) and (12) is proportional to

$$(79) \qquad \int F(y)(1 - kF'(y)r^{1/2}) \, dy,$$

where the integration is over the values of y on the characteristics which are not cut off by shocks before reaching this value of r. If the limits were 0 and ∞, i.e. if the integration were over *all* the characteristics, its value would be 0; hence (79) may be replaced, with its sign reversed, by the integral over the characteristics previously excluded. This integral vanishes by use of equations (51) and (52); hence to this first approximation the mass flux is zero. There is no second approximation to the theory but it is expected, as in Lighthill's work on Friedrichs' theory, that to a second approximation there would be a net mass outflow far from the axis to balance the reduced mass flow behind the projectile due to increased entropy, and then to achieve the balance it would be necessary to include the third order pressure waves reflected from the front shock and transmitted through the rear one.

In the expression (78) for the drag, $e - e_0 + p_0(\rho^{-1} - \rho_0^{-1})$ may be replaced by $T_0 S$, where T_0 is the temperature in the main stream and S is the difference of the entropy from its main stream value. It is easily seen that between the shocks, the wave energy is proportional to (amplitude)^2 $\times$ wave length $\times$ $r \propto r^{-3/2} \times r^{1/4} \times r = r^{-1/4}$ which tends to zero as the plane Π tends to infinity

downstream. In the tail the contribution to the wave energy, apart from the entropy term, is proportional to

$$\int_0^r \frac{1}{r(x-\alpha r)^3}\, r\, dr = O(r^{-1/2}), \tag{80}$$

which also tends to zero, hence

$$D = \int_0^\infty 2\pi\rho_0 T_0 S r\, dr. \tag{81}$$

The integral (81) is over a plane downstream of the body, but since entropy is conserved, being constant along the stream-lines, the integral of the entropy jump over the shocks may be taken instead. If Δp is the jump in pressure at a shock, $S = c_v(\gamma^2 - 1)(\Delta p/p_0)^3/12\gamma^2$ where c_v is the specific heat at constant volume; hence, using (67) and that $c_v T_0 = a_0^2/\{\gamma(\gamma-1)\} = U^2/\{M^2\gamma(\gamma-1)\}$, the expression for the drag becomes

$$D = \frac{\pi\rho_0 U^2 k}{12} \int \{F(y_2) - F(y_1)\}^3 r^{-1/2}\, dr, \tag{82}$$

where the integral must be taken over all shocks. From (61), $\frac{1}{2}kr^{-1/2}\, dr = d\{(y_2 - y_1)/[F(y_2) - F(y_1)]\}$; hence,

$$\begin{aligned}\frac{D}{\pi\rho_0 U^2} &= \frac{1}{6}\int \{F(y_2) - F(y_1)\}^2 (dy_2 - dy_1) \\ &\quad - \frac{1}{6}\int (y_2 - y_1)\{F(y_2) - F(y_1)\}\, d\{F(y_2) - F(y_1)\}.\end{aligned} \tag{83}$$

After a certain amount of manipulation and use of (60), it is found that the contribution to (83) of any single portion of shock is

$$\begin{aligned}&\int F^2(y_2)\, dy_2 - \int F^2(y_1)\, dy_1 \\ &\quad - \tfrac{1}{3}\,[\{F^2(y_2) + F^2(y_1) + F(y_1)F(y_2)\}(y_2 - y_1)],\end{aligned} \tag{84}$$

where $[\cdots]$ denotes the difference in the values at the ends of the portion. Now apply this to all the shocks in such a way that the end points of any portion are: (a) the starting point of the shock or (b), the point where the shock joins others or (c), the point at infinity on the shock, and consider the total value of $[\cdots]$. The contribution from starting points is zero since there $y_2 = y_1$ even if the shock is attached. The contribution from a join of shocks is zero. For, suppose the values of y_1 and y_2 at the join for the two "incident" shocks are (Y_1, Y_2) and (Y_2, Y_3) respectively, then the values of y_1 and y_2 for the "continuing" shock are (Y_1, Y_3), and the total contribution in $[\cdots]$ from this join is proportional to

$$\sum \{F^2(Y_2) + F^2(Y_1) + F(Y_1)F(Y_2)\}\{F(Y_2) - F(Y_1)\},$$

since $Y_2 - Y_1 = k^{-1}r^{-1/2}\{F(Y_2) - F(Y_1)\}$ etc. with a common value of r (the sum is for the three pairs of suffixes (1, 2), (2, 3) and (3, 1)); this sum is zero. The contribution as the point on a shock tends to infinity is also zero since for the rear shock $y_1 \to y_0$, $y_2 \to \infty$, $y_2(y_1 - y_0) = O(1)$, $F(y_2) = O(y_2^{-3/2})$, $F(y_1) \sim (y_1 - y_0)F'(y_0)$, and the front shock may be treated similarly. Hence the total contribution of $[\cdots]$ is zero, and (83) and (84) give

$$D = \pi\rho_0 U^2 \int_0^\infty F^2(y)\, dy. \tag{85}$$

This is a very simple form for the drag; it is given directly in terms of the fundamental function $F(y)$ associated with the flow, and moreover, it may be easier in computations to use this form instead of the usual von Kármán double integral. It may be reduced to the von Kármán form; for, if $F(y)$ is replaced by

$$\int_0^y \frac{f'(t)\, dt}{\sqrt{y - t}} \tag{86}$$

and the integration over y performed, (85) becomes

$$D = \pi\rho_0 U^2 \int_0^\infty \int_0^\infty f'(t)f'(\tau) \log \frac{1}{|t - \tau|}\, dt\, d\tau, \tag{87}$$

assuming that the ultimate radius of the body is finite so that $f(t) = O(t^{-1})$ for large t. This expression for the drag contains more than the drag D_1 on the projectile alone, which would be given by (87) with the upper limits replaced by l, the length of the body. If $F_1(y)$ is the F function for the same projectile but with a wake of uniform cross-section equal to that of the base, then

$$D_1 = \pi\rho_0 U^2 \int_0^\infty F_1^2(y)\, dy. \tag{88}$$

The extra drag $D - D_1$, which is due to the thinning of the wake, must be part of the base drag; presumably it is the contribution of the base pressure on the annulus of the base, which is the difference of the base cross-section and the ultimate cross-section of the wake. But the base pressure is roughly constant: hence an approximate value of the total base drag is suggested to be

$$D_B = \frac{R_B^2}{R_B^2 - R_W^2}(D - D_1), \tag{89}$$

where R_B and R_W are the radii of base and wake respectively.

The physical significance of D is that it is all that part of the drag which is associated with the degradation of energy of the shocks rather than with loss of energy in the boundary layer and the wake.

Appendix. Two-Dimensional Steady and One-Dimensional Unsteady Flows

In general, as explained in Part 1, the Friedrichs theory does not describe a shock which is formed *inside* a disturbed region of the flow. Such shocks, however, are of scientific and practical interest since they occur (a) in the problems of accelerating and oscillating pistons, (b) in flow past an aerofoil (or wall) which has compression regions other than the simple discontinuities at the leading and trailing edges, and (c) where a boundary layer or wake is producing compression waves in the stream. An example of the latter occurs when a body with a leading edge of finite thickness is placed in a supersonic stream. Apart from the main (detached) shock, a second much weaker shock is observed, if the Reynolds number is large enough, just behind the edge. The explanation which is given for this phenomenon is that the flow separates leaving a small bubble of air at the edge. The bubble and the edge of the boundary layer outside it will be shaped rather like a blunt nosed aerofoil cusped at the trailing edge; the shock is produced by the *continuous* compression at the rear. The present theory may be used to relate the shape of the bubble (which may be invisible for a very thin leading edge) with the visible shock.

The first order theory for two-dimensional flow (referred to as I) past *any* boundary whose slope is always small, although not necessarily continuous, and that for the one-dimensional unsteady flow (referred to as II) produced by *any* small piston motion, will now be set out. It is convenient to use the same notation as in the projectile problem and it is hoped that the use of y for the characteristic variable will not prove inconvenient in comparing the theory with other work. In I, x and r are, respectively, the distances along and perpendicular to the boundary wall $r = R(x)$, the undisturbed velocity is U with Mach number $M = U/a_0$, and the disturbed potential is $Ux + U\phi$. The linearized solution of the equations of motion is, as is well-known, that ϕ is a function of $x - \alpha r$, where $\alpha = \sqrt{(M^2 - 1)}$, hence

$$u = \phi_x = -F(x - \alpha r)/\alpha, \qquad v = \phi_r = F(x - \alpha r) = -\alpha u, \tag{90}$$

and the arbitrary function F is determined from the boundary condition that

$$v = R'(x) \qquad \text{on} \qquad r = R(x). \tag{91}$$

Modifying the solution in accordance with the hypothesis of Part 2, a uniformly valid solution of the flow is,

$$u = -F(y)/\alpha, \qquad v = F(y), \tag{92}$$

where y is determined from the condition that $y =$ constant is a characteristic curve. From (9) and (92) the characteristics are

$$x = \alpha r - kF(y)r + kF(y)R(y) + y, \qquad y = \text{constant}, \tag{93}$$

where $k = \frac{1}{2}(\gamma + 1)M^4/\alpha^2$ and, as before, y is defined uniquely as the value of $x - \alpha r$ at the boundary. The flow is described then by (92) and (93); from (91), $F(y)$ is equal to the slope of the boundary at the point where it is met by the characteristic y, that is, $F(y) = R'(X)$ where $X(y)$ is determined by $X - \alpha R(X) = y$; if $R'(x)$ is continuous, $F(y)$ may be approximated as $R'(y)$. This solution is exactly the first approximation to the simple wave.

In problem II, if r denotes distance in the direction of the piston motion, if x denotes time, if the piston curve is given by $r = R(x)$ and if the potential is ϕ, exactly the same results are obtained except that α is now a_0^{-1}, where a_0 is the undisturbed speed of sound, and k is $\frac{1}{2}(\gamma + 1)/a_0^2$; the function $F(y) = R'(X)$ is, of course, the velocity of the piston when the "wavelet" defined by y left it. The results are found in a way similar to that above; the linearized theory has the same form and the characteristics are given by $dr/dx = a + v$ where the local speed of sound, a, is given by the Bernoulli equation $u + \frac{1}{2}v^2 + a^2/(\gamma - 1) = a_0^2/(\gamma - 1)$. Thus both problems are solved by (92) and (93), and the development below may be applied to either problem.

In a region where $F'(y) > 0$, the characteristics run together to form a limit line; in any such region there must be a shock to cut off the characteristics before they meet each other. The shock is determined from the "angle property" (which applies in the (x, r) plane for I and in the (a_0x, r) plane for II) as in the projectile problems. For a "front shock," or at a large distance from the boundary on any shock, the characteristics (93) may be approximated as

$$x = \alpha r - kF(y)r + y, \qquad y = \text{constant}, \tag{94}$$

and the shock $x = \alpha r - G(r)$ is given by

$$\int_{y_1}^{y_2} F(y)\,dy = \tfrac{1}{2}(y_2 - y_1)\{F(y_1) + F(y_2)\}, \tag{95}$$

$$\frac{1}{kr} = \frac{F(y_2) - F(y_1)}{y_2 - y_1}, \tag{96}$$

$$G = kF(y_1)r - y_1 . \tag{97}$$

The description of the shocks from the F-curve by means of the "equal area segments" is carried out as for the projectile except that the gradient of the segment is now $(kr)^{-1}$; the technique has already been given in detail. If there is an attached shock due to a compressive discontinuity of slope in the boundary, slight modifications are required as before; (93) may be approximated everywhere on the shock by $x = \alpha r - kF(y)(r - R_1) + y$, where R_1 is the value of $R(x)$ at the discontinuity, and the shock is given by (95), (96) and (97) but with r replaced therein by $r - R_1$. From Bernoulli's equation, the strength of the shock is

$$s = \frac{\gamma M^2}{\alpha}\{F(y_2) - F(y_1)\} \tag{98}$$

in I, and

$$s = \gamma\alpha\{F(y_2) - F(y_1)\} \tag{99}$$

in II.

The determination of the shocks completes the description of the flow, and the general theory may now be applied to any of the problems mentioned above. The full details of these will not be given here (because in view of the work on the projectile it is obvious how to proceed), but comments will be made upon some interesting points which have not arisen before.

For the aerofoil problem solved by Friedrichs, the front and rear shocks each have undisturbed flow on one side of them. Hence, in each case, one of y_1 and y_2 may be eliminated in the shock equations to give G and r in terms of a single parameter; the expressions obtained agree with the first terms of Friedrichs' results. The upper and lower sides of the aerofoil must be treated separately of course; consider in particular the upper side. The type of F-curve is shown in Figure 14. It is of interest to note that the (algebraic) area under the F-curve

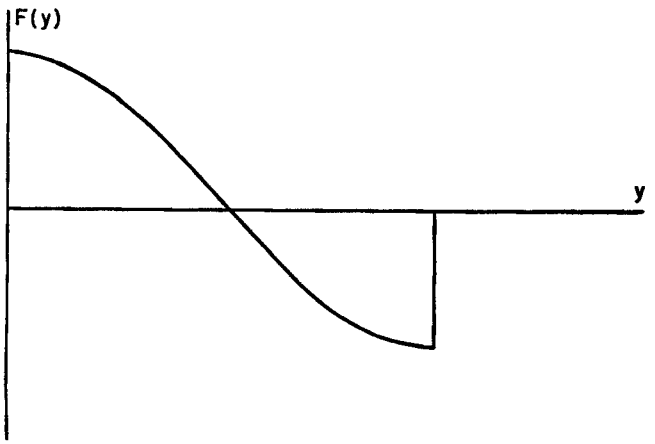

FIGURE 14

(which was always zero for the projectile) is $R(l)$, where the origin of co-ordinates is at the leading edge and the trailing edge is at $x = l$; hence the two shocks balance only if $R(l) = 0$. This is intimately connected with the lift since it may be shown, by the methods of Part 7, that the contributions to the lift and drag from the upper side of the aerofoil are

$$L = \frac{\rho_0 U^2}{\alpha}\int_0^\infty F(y)\,dy, \qquad D = \frac{\rho_0 U^2}{\alpha}\int_0^\infty F^2(y)\,dy; \tag{100}$$

similar results are obtained for the lower side. Hence, to this order, the lift is proportional to $R(l)$, a result which is already well-known.

In the problem of a piston which is accelerated from the rest position

$r = x = 0$, it is supposed that the acceleration ceases to be positive after a finite time, $x = x_0$ say, so that $R'(x)/a_0$ remains small. The subsequent piston motion plays an important part in the behaviour of the shocks after its formation by the initial compression region, but introduces nothing new. After x_0 , $R'(x)$ does not increase and for definiteness it is assumed to remain constant. (If the acceleration does continue indefinitely, the theory applies only to the initial region). The three fundamental types of F-curve to be considered are shown in Figure 15; they are the cases where the acceleration (i) decreases, (ii) remains

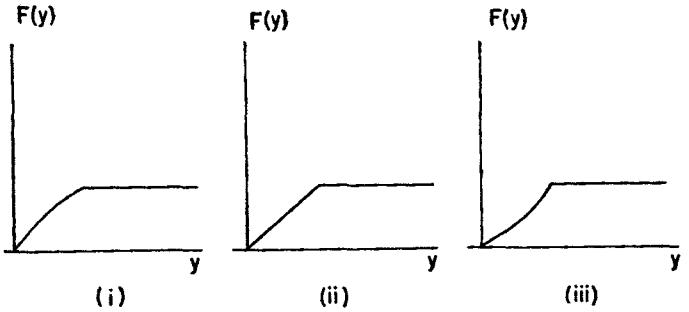

FIGURE 15

constant, and (iii) increases. Interpreting these by the "equal area segments," it is seen that in (i) the shock starts with zero strength on the first characteristic $y = 0$, in (ii) all the characteristics from the compression intersect in a single point and the shock starts there with finite strength, and in (iii) the shock starts with zero strength on the final characteristic $y = x_0 - \alpha R(x_0)$. The result in (ii) may appear surprising at first sight since in reality it is clear that a shock can only start in the fluid with zero strength. The explanation is that this first order theory only measures the dominant term which is $O(\delta^{-1})$ (where δ is the maximum value of $R'(x)/a_0$ say), in the expressions for distances along a shock. For a uniformly accelerated piston, the shock reaches its maximum strength, which is proportional to δ, in a distance $O(1)$ which is ignored in this theory. It is interesting that in these problems of shock formation the rate of increase of shock strength is greater (being $O(\delta)$) for (ii) than for (i) or (iii) in which it is $O(\delta^2)$. More complicated F-curves with points of inflexion resulting in shock formation inside the wave, or with more than one shock may be treated in a similar way by the methods of Part 4.

If the piston oscillates periodically, then, in theory and perhaps sufficiently closely in practice, the F-curve is periodic. Suppose one period has the simple form shown in Figure 16. The shock starts at the point of inflexion, strengthens and ultimately decays. Now the integral of F in this period is zero, because R returns to its initial value at the end of the period, hence as $r \to \infty$ on the shock $y_1 \to 0+$ and $y_2 \to Y-$ where Y is the value of y at D. The straight characteristics from 0 and D reach to infinity and the flow between them is independent of

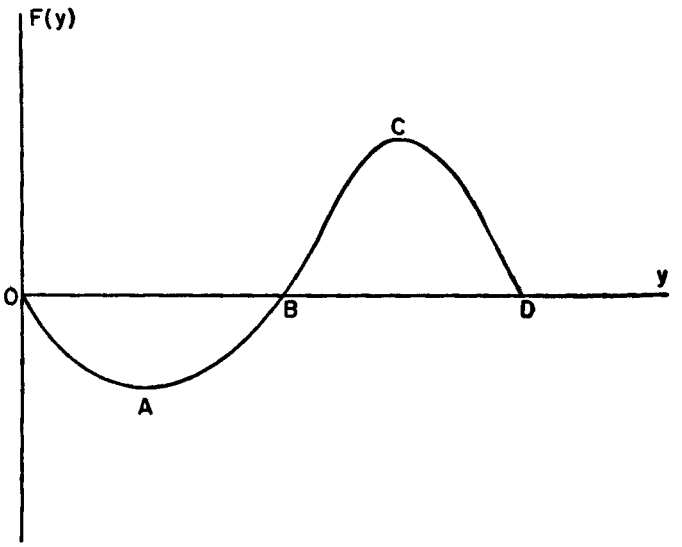

FIGURE 16

the flow outside. The decay of the shock at infinity may be determined from the shock equations using the approximations for y_1 and y_2 near 0 and D, respectively, to give

$$G(r) = -\frac{1}{2}Y + \left\{\frac{1}{8}\frac{F''(0)}{F'^2(0)}Y^2 - \frac{Y}{F'(0)}\right\}(kr)^{-1}. \tag{101}$$

(In this expression it has been assumed, for simplicity, that $F'(0) = F'(Y)$ and $F''(0) = F''(Y)$). The first term in the expression for the strength is found immediately from (96) and (98) as

$$s = \gamma\alpha\frac{y_2 - y_1}{kr} \simeq \frac{\gamma\alpha}{k}\frac{Y}{r} = \frac{2\gamma}{\gamma+1}\frac{a_0 Y}{r}. \tag{102}$$

This result is of considerable interest since it shows that the strength of the shock at large distances depends only on the period of oscillation (Y) of the piston motion and is independent of its particular form. It fits in with the previous results, however, because, in one dimensional unsteady flow, the result analogous to (71) is that the pressure ratio p/p_0 falls linearly with time at a rate $2\gamma a_0\{(\gamma+1)r\}^{-1}$ which is independent of the piston motion; for the periodic motion, the time between the shocks must be Y hence the strength $\Delta p/p_0$ must be the product given in (102).

Practical use may be made of (102) (possibly in astronomy) since if the period of oscillation is known together with the values of γ and a_0, a measure of the strength of the shock determines the distance from the source. From this point of view, the analogous formula for the shocks produced by the oscilla-

tions of a sphere may be preferable. It may be obtained in the same way, using the results of the author's paper [7], and is very similar; it is

$$s = \frac{2\gamma}{\gamma + 1} \frac{a_0 Y}{r \log r}. \tag{103}$$

GRAPHS

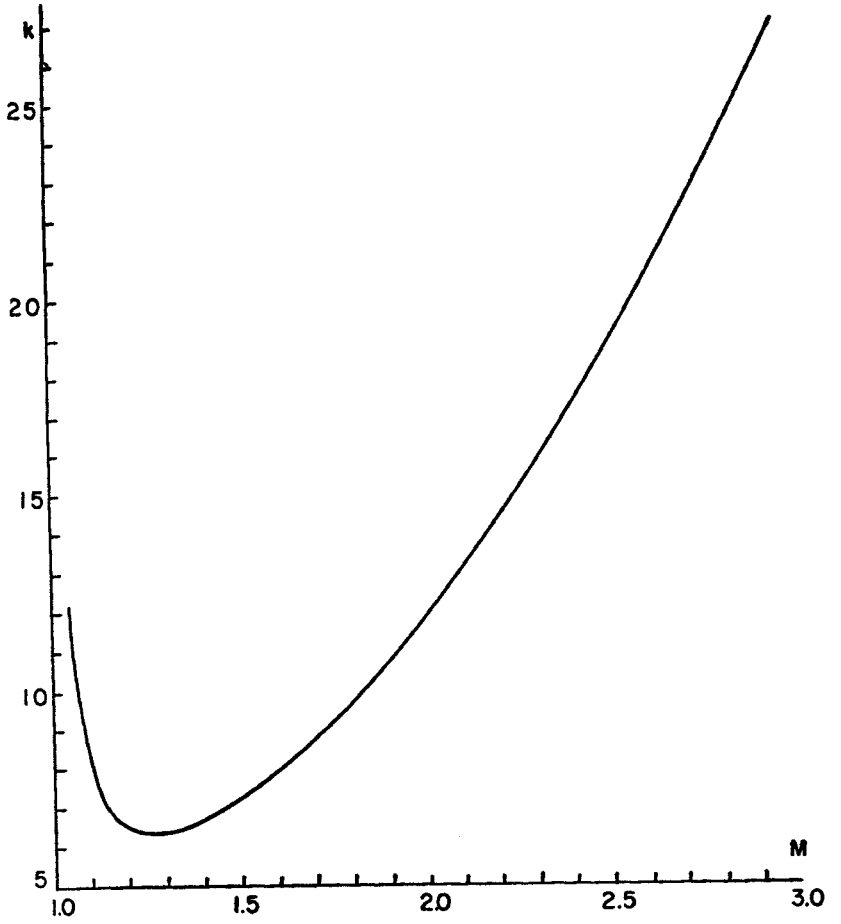

Variation of k with Mach number M.

GRAPH A

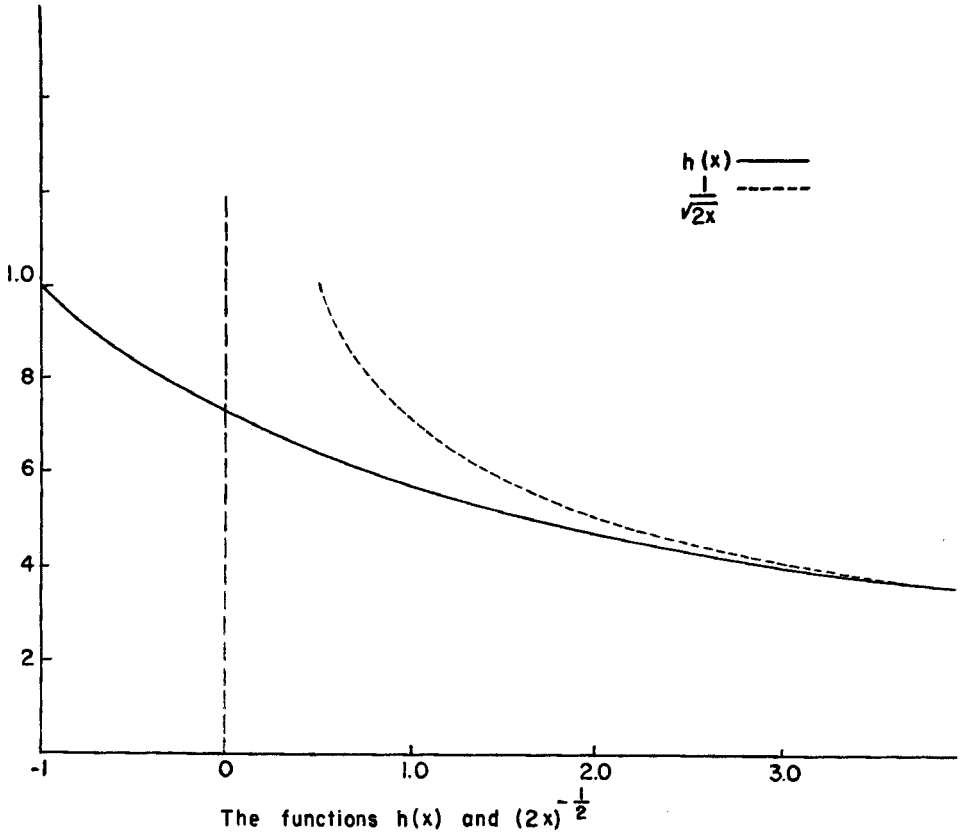

The functions $h(x)$ and $(2x)^{-\frac{1}{2}}$

GRAPH B

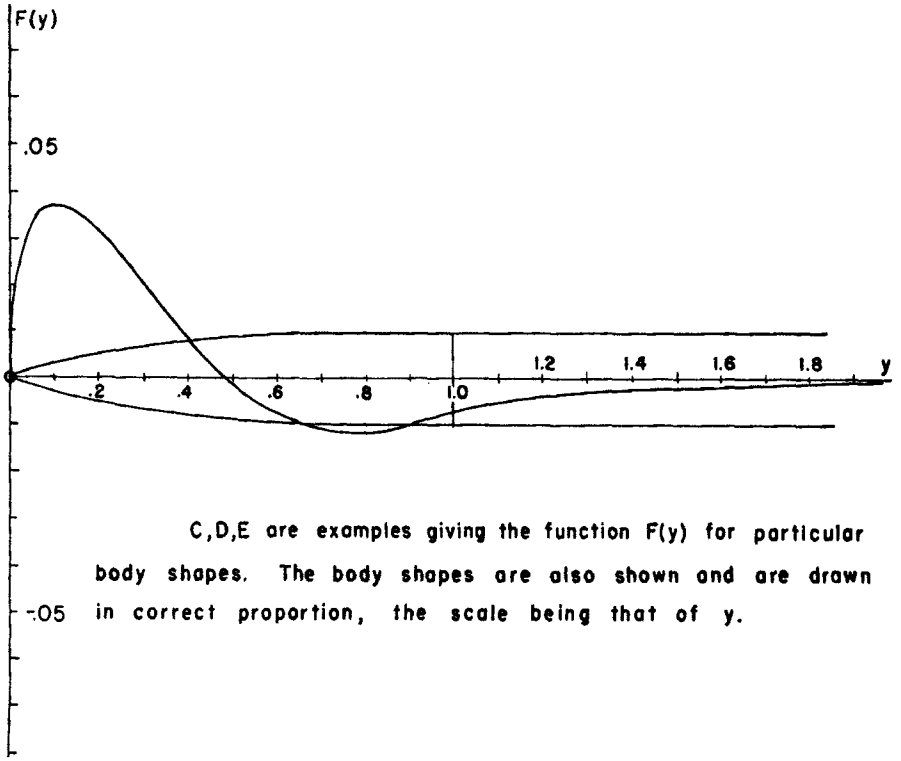

C,D,E are examples giving the function F(y) for particular body shapes. The body shapes are also shown and are drawn in correct proportion, the scale being that of y.

GRAPH C

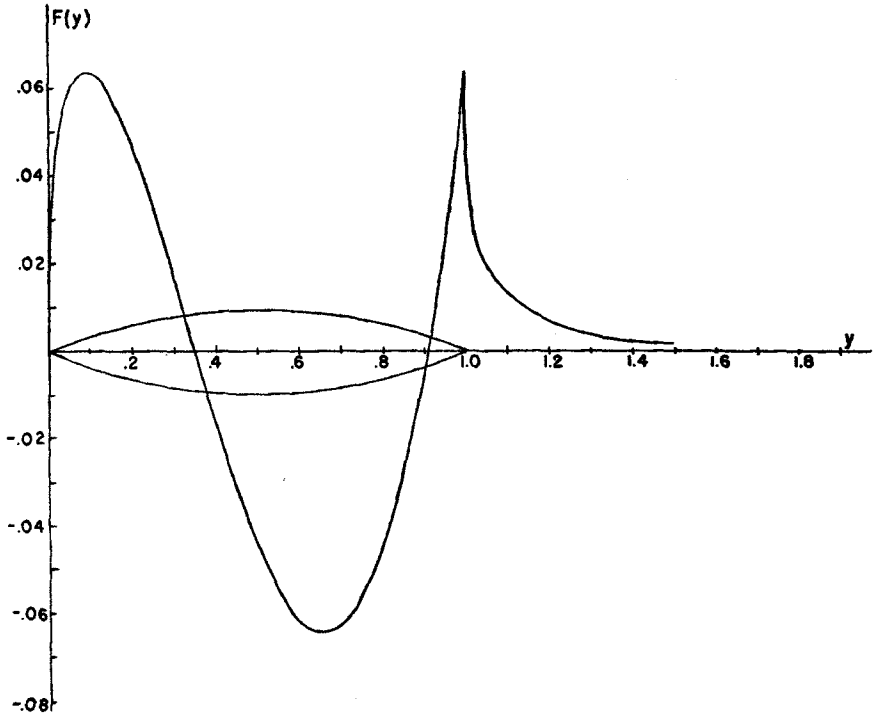

GRAPH D

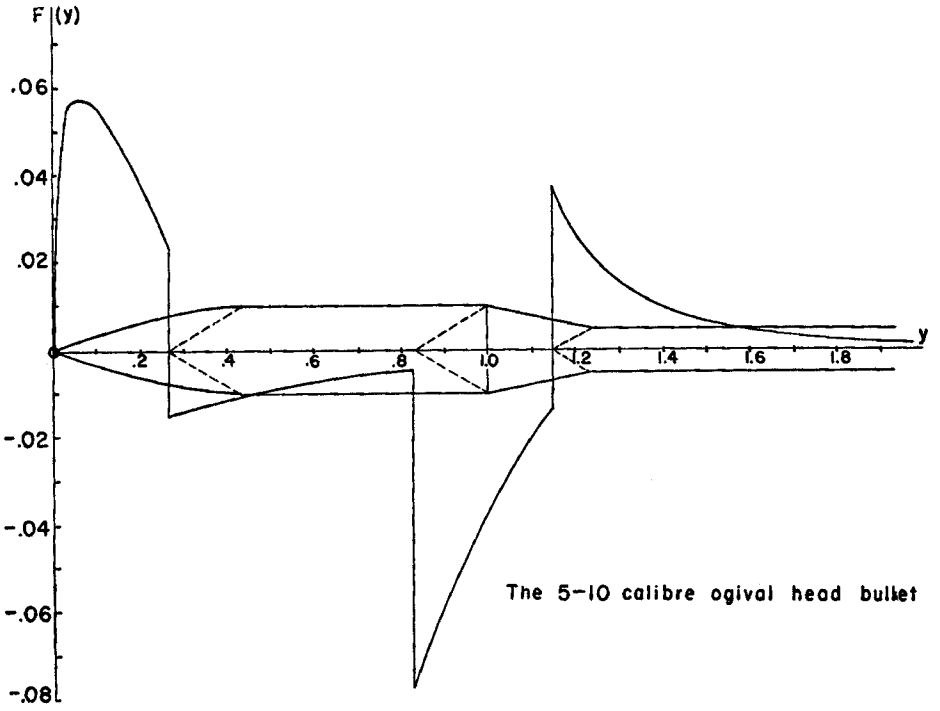

GRAPH E

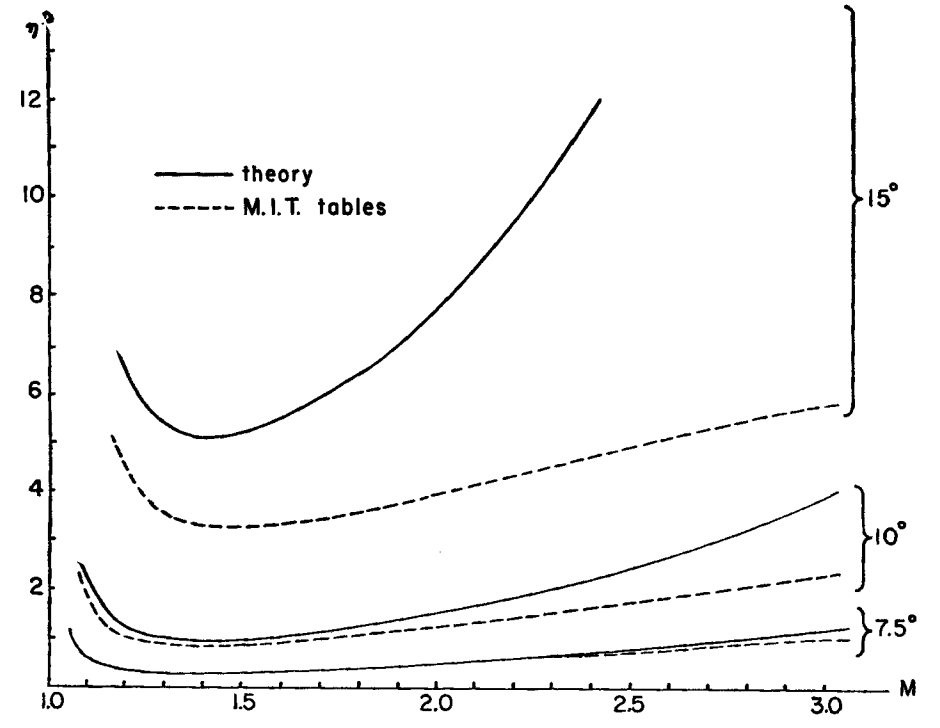

GRAPH F

Curves showing the variation of η with M for cones of semiangle 7.5°, 10° and 15°, and comparison with numerical results.

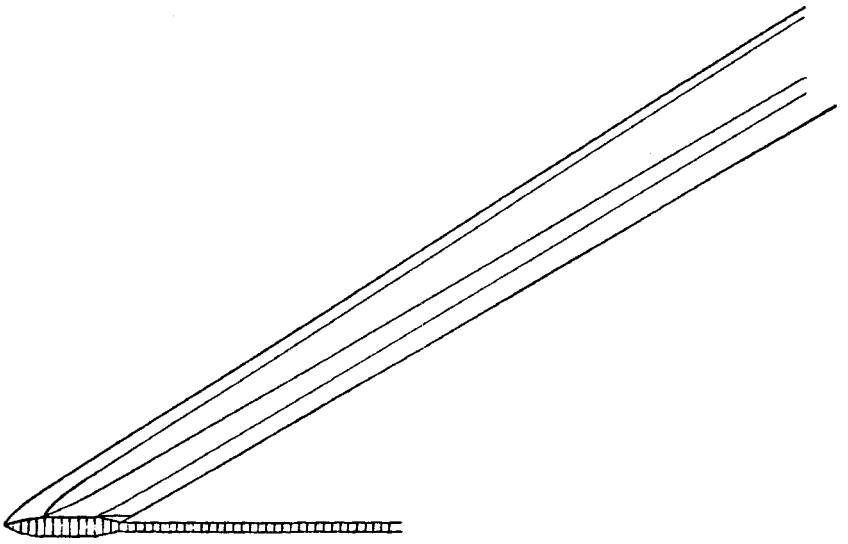

The flow pattern for the ogival head bullet.

GRAPH G

The author wishes to thank Professor M. J. Lighthill for his interest, encouragement and helpful criticism throughout the preparation of this paper.

BIBLIOGRAPHY

[1] Friedrichs, K. O., *Formation and decay of shock waves*, Communications on Pure and Applied Mathematics, Volume I, No. 3, 1948, pp. 211–245.

[2] Lighthill, M. J., *The energy distribution behind decaying shocks*, Philosophical Magazine, Series 7, Volume 41, 1950, pp. 1101–1128.

[3] Lighthill, M. J., *Supersonic flow past bodies of revolution*, Aeronautical Research Commission, Reports and Memoranda, London, No. 2003, 1945.

[4] Broderick, J. B., *Supersonic flow round pointed bodies of revolution*, Quarterly Journal of Mechanics and Applied Mathematics, Volume II, Part I, 1949, pp. 98–120.

[5] Whitham, G. B., *The behaviour of supersonic flow past a body of revolution, far from the axis*, Proceedings of the Royal Society, Series A, Volume 201, 1950, pp. 89–109.

[6] Ward, G. N., *Supersonic flow past slender pointed bodies*, Quarterly Journal of Mechanics and Applied Mathematics, Volume II, Part I, 1949, pp. 75–97.

[7] Whitham, G. B., *The propagation of spherical blast*, Proceedings of the Royal Society, Series A, Volume 203, 1950, pp. 571–581.

[8] Lighthill, M. J., *A technique for rendering approximate solutions to physical problems uniformly valid*, Philosophical Magazine, Series 7, Volume 40, 1949, pp. 1179–1201.

[9] Lighthill, M. J., *Supersonic flow past slender bodies of revolution the slope of whose meridian section is discontinuous*, Quarterly Journal of Mechanics and Applied Mathematics, Volume I, Part I, 1948, pp. 90–102.

[10] Lighthill, M. J., *The position of the shock-wave in certain aerodynamic problems*, Quarterly Journal of Mechanics and Applied Mathematics, Volume I, Part 3, 1948, pp. 309–318.

[11] Broderick, J. B., *Supersonic flow past a semi-infinite cone*, Quarterly Journal of Mechanics and Applied Mathematics, Volume II, Part I, 1949, pp. 121–128.

[12] Massachusetts Institute of Technology, *Technical Report No. 1, Tables of Supersonic Flow Around Cones*, The Murray Printing Co., Cambridge, Massachusetts, 1947.

[13] DuMond, J. W. M., Cohen, E. R., Panofsky, W. K. H., and Deeds, E., *A determination of the wave forms and laws of propagation and dissipation of ballistic shock waves*, Journal of the Acoustical Society of America, Volume 18, 1946, pp. 97–118.